MACHINE VISION SYSTEMS: AUTOMATED INSPECTION & METROLOGY

By

Benjamin Antonio Guardiola

A Thesis
Submitted to the
Faculty of the Graduate School
of
Western Carolina University
in Partial Fulfillment of
the Requirements for the Degree
of
Master of Science

Committee:

_____ Director

_____

_____

_____ Dean of the Graduate School

Date:_____

Fall 2009
Western Carolina University
Cullowhee, North Carolina

MACHINE VISION SYSTEMS: AUTOMATED INSPECTION & METROLOGY

A thesis presented to the faculty of the Graduate School of
Western Carolina University in partial fulfillment of the
requirements for the degree of Master of Science in Technology

By

Benjamin Antonio Guardiola

Director: Dr. Aaron K. Ball
Associate Professor of Engineering & Technology
Engineering & Technology Department

Committee Members: Dr. Wesley L. Stone, Engineering & Technology
Dr. Robert Anderson, Engineering & Technology

September 2009

TABLE OF CONTENTS

LIST OF TABLES

LIST OF FIGURES

ABSTRACT

MACHINE VISION SYSTEMS: AUTOMATED INSPECTION & METROLOGY

Benjamin Antonio Guardiola, M.S.

Western Carolina University (September 2009)

Director: Dr. Aaron K. Ball

The purpose of the project was to develop a high speed, high accuracy measuring device to aid the engineering technology department at Western Carolina University. When something requires measurement with a high degree of accuracy a coordinate measuring machine is used. This process can be very time consuming especially when multiple iterations are required. A machine vision system is capable of making the same type of measurements in a matter of seconds rather than minutes.

This study covers the development and testing of a machine vision system. Several tests were conducted to help develop and improve the system through changes to the test fixture, lighting, programming, and test object. The results of these tests are only valid for the specific set-up and equipment used, and cannot be transferred to any other system. Even slight changes to the equipment during testing showed significant changes in the data being gathered. This contributed to the final conclusion that the measurements gathered by the machine vision system are not comparable to those of the coordinate measuring machine at any level of accuracy. Improvements to the machine vision system setup must be made to improve accuracy.

CHAPTER ONE: STATEMENT OF THE PROBLEM

This project aims to evaluate the ability of a Keyence Machine Vision System (MVS) to accurately measure linear dimensions using a Zeiss Coordinate Measuring Machine (CMM) as a reference. A baseline test setup to use for the Keyence MVS was first determined through preliminary experimentation. The accuracy of the Keyence MVS was then evaluated alongside the Zeiss CMM through measurements gathered using the most appropriate test setup.

OBJECTIVES

This project, using a Machine Vision System (MVS), examines linear inspection methods and evaluates their accuracy, compared to a Coordinate Measuring Machine (CMM). The goal of this project is to determine the capabilities and limitations of the MVS when used for metrology. To assess these attributes, a test part was produced with four circular pockets of varying size for measurement and served as the test part for both systems.

The test part is divided into eight features as shown in Figure 1 below. The features were measured with a Zeiss Contura G2 (HTG) CMM and a Keyence MVS.

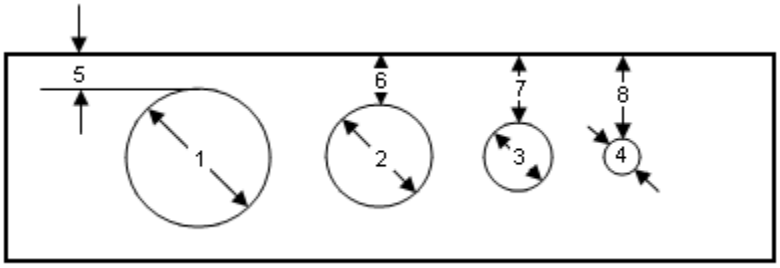

Figure 1 – Test Part

The gathered data was then used to determine a formula to convert pixels, the output of the MVS, into inches, the output of the CMM. The accuracy of the MVS measurements relies on the accuracy of the pixel conversion formula (found in the Data Gathering Procedures section), which assumes that the CMM measurements are accurate.

BACKGROUND AND NEED FOR THE STUDY

Machine Vision is a subfield of engineering that encompasses computer science, optics, mechanical engineering, and industrial automation. Most MVSs require digital input/output devices and computer networks to control other manufacturing equipment, such as robotic arms. Some uses of MVSs include part identification, defect inspection, presence/absence detection, dimensional measurement, positioning, and counting. One of the most common applications of MVSs is the inspection of manufactured goods, such as semiconductor chips, automobile parts, food and pharmaceuticals. Just as human inspectors working on assembly lines visually inspect parts to judge the quality of workmanship, MVSs use digital cameras, smart cameras and image processing software to perform similar inspections.

Another common use of MVSs is dimensional measurement or metrology. The standard metrological instrument for applications requiring extreme accuracy is the CMM. The most skilled CMM operators require more than a minute to accurately measure any given object. Most Machine Vision Systems are attached to high-speed conveyors, and the Keyence system used for this project consistently reads under 250ms (based on a

previous “Pattern Sort” program). According to the Keyence Corporation, the machine vision system used for this project is capable of image transfer times of 16ms (Keyence, 2006). This time can be reduced to 3ms when set to “partial image read.” Most MVSs are attached to high-speed conveyors, which would not allow for the time needed to properly run a CMM. In order to utilize a CMM, a part would have to be removed from the conveyor and inspected, which would not allow for 100% inspection. Examining every part results in superior data that generates higher quality parts.

The MVS being used is a Keyence CV-3002 Series: Multi-camera Universal Machine Vision System, with a CV-035M Series: Double Speed Digital Camera (Monochrome). The CMM being used is a Zeiss Contura G2 (HTG) (High Temperature Gradient). This machine is a bridge-type CMM. According to the manufacturer, this machine has an accuracy of ± 2µm (Carl Zeiss, 2008). If equal accuracy can be demonstrated between the two systems, cycle times of production can be significantly reduced yielding reduced lead times for part production quantities.

SIGNIFICANCE OF THE STUDY

This project analyzes the accuracy of the Keyence MVS when used to measure the diameter of circular holes, using diametrically opposing points. The project institutes a set of standards to use for this type of measurement when programming the Keyence MVS. Establishing a tested and verified process benefits Western Carolina University by

validating future work performed using these guidelines and has implications for improving production cycle times in industrial settings.

One of the greatest benefits to utilizing a MVS is the capability to inspect 100% of the parts under evaluation. The process of inspection, as Deming wrote, is an information-gathering tool for improvement (Evans et al, 2005). Another quality pioneer, Juran, stated that in order to control quality, one must determine what to control, establish units of measurement to evaluate data, establish a standard of performance, measure actual performance, interpret the difference between standard and actual performance, and take action on the difference (Evans et al, 2005). Both Deming and Juran agree that the key to achieving superior quality is to identify and reduce sources of variation. The end goal of any organization should be achieving a Six Sigma level of quality (3.4 errors or defects per million opportunities), which involves reducing the amount of variation in a process and correcting processes that create errors or defects (Evans et al, 2005).

The outcomes of this research study have the potential to reduce costs, improve cycle times and achieve 100% inspection for various types of components and manufactured goods.

DEFINITIONS AND KEY TERMS

Analysis of Variance – (ANOVA) – a statistical tool for analyzing data that examines the difference between two or more means by comparing the variance within groups and between groups

Automation – the techniques and equipment used to achieve automatic operation or control.

Charge-coupled Device – (CCD) – an analog shift register, most widely used for parallel signals of photoelectric light sensors, which convert an optical image into electrical signals. Generally known as a type of image sensor, although it technically only refers to how the image signal is output.

Computer Numerical Control – (CNC) – an automation based control system that utilizes numerical values to represent desired positions and/or tools. This system allows for accurate and repeatable machine movements. In machining operations, it allows for optimized feeds, speeds, and cycle times to be programmed.

Coordinate Measuring Machine – (CMM) – a machine used to measure geometrical characteristics of an object. The machine utilizes a probe that moves about a three-axis grid (x,y,z) and touches various spots on the object being measured. The coordinates gathered by touching the part are then used to determine the size and position of the object. These machines are considered to be extremely accurate.

Design of Experiments – (DOE) – a structured, organized method for determining the relationship between factors (Xs) affecting a process and the output of that process (Y).

Double Speed Digital Camera – a camera that scans horizontal and vertical at frequencies double the speed of a standard camera. These cameras boast double the image-capture speed and are designed for industrial applications.

F-test – a statistical tool used to test if the standard deviations of two populations are equal.

Keyence – The Keyence Corporation is the leading supplier of sensors and measuring instruments for factory automation applications.

Luminous flux – “Luminous power” – the measure of the perceived power of light. The unit of measurement is the Lumen (lm).

Lux – is the unit of measurement for illuminance (light on a surface) and luminous emittance (light reflected from a surface). Lux is calculated by dividing the number of lumens by the square meters the light is spread over.

- Lux = lm / m^2

Machine Vision System – (MVS) – a system that features a camera or image capture device and a form of image processing software that work together to perform narrowly defined tasks such as counting or defect inspection. They are preferred for visual inspection, especially applications that require high-speed, high-magnification, 24-hour operation, and/or repeatability of measurements.

Metrology – the science of measurement; the use of standards and methods for measurement, quality control, and instrument calibration.

– Work performed regarding the development and use of measurement standards and methods, old and new. The results of these actions must be repeatable in order to establish a comparison between the measuring instrument, or method, and the established standard.

MVS Inspection Tools – the following are the MVS inspection tools being examined:

Edge Width

- This inspection tool detects edges in the current image and measures the distance between edges. It can be used to measure features or distance between parts. The edges are defined by transitions from light to dark. The

program allows the user to indicate which transition to detect, allowing for measurement of “Inner”, “Outer”, and “Specified” gaps (Keyence, 2006).

Pattern Sort – “Variable Search”

- This inspection tool requires that images of targets are registered and stored in the MVS memory. Registered images can be stored in groups, which is useful when targets vary in size or shape. The current image is compared to the stored images. The program outputs the number of targets for each group and the correlation value. The position and angle of each target can also be output (Keyence, 2006).

Optics – the science of light. It is a branch of physics that deals with the properties and behavior of light and its interaction with matter.

Pixel – “Picture Element” – the smallest unit that makes up an image. An image is composed of an organized array of pixels or dots.

Six Sigma – a data-driven approach and methodology for eliminating defects in any process: from manufacturing to transactional and from product to service. The process strives to reach six standard deviations between the mean and the nearest specification limit.

Tolerance – the difference between the upper specification limit and the lower specification limit.

Variance – σ^2 – a way to quantify the distance between an iteration (X) and the mean (μ) of the data set. Variance is defined as the sum of this distance squared divided by the total number of iterations (N). This is displayed in the equation below.

$$\sigma^2 = \frac{\Sigma(X - \mu)^2}{N}$$

Zeiss – Carl Zeiss Industrial Metrology is the world's leader in CNC measuring machines and complete solutions for multidimensional metrology in the metrology lab and production.

Zeiss Contura G2 (HTG) CMM – (High Temperature Gradient) this is a bridge-type CMM with an accuracy of ± 2µm. The HTG provides the same accuracy as the regular version over a larger temperature range.

DELIMITATIONS OF THE STUDY

This section discusses the depth and limitations of the project along with the particular methods and tools that were used to complete it. A brief discussion of the difficulties in ascertaining the accuracy of the data gathered is also included.

The research and findings of this study are restricted to a Keyence MVS. The results may not be transferrable to other similar vision systems, and any modification of the vision system's setup may alter the results. The camera jig used for this experiment was

designed for overhead inspection of parts on a conveyor. The camera was positioned perpendicular to the target object. The camera should not be operated in environments above 122°F, so a thermometer was attached to the camera to ensure the camera was not being harmed. Two clamp lights were attached on each side of the camera. These lights were positioned to provide front, bright-field, diffuse illumination. The lights feature a 10.5” aluminum reflector, an Edison socket, and 250watt maximum capacity (each). The metrological benchmark used for this study was a Zeiss Contura CMM. Variation may exist across other manufactured CMM systems, and inference to other equipment cannot be made. Further research is needed to determine if these results are shared with similar systems.

The test part implemented in this research was student fabricated and was not certified to be within a predetermined tolerance. The findings are only relevant to the specific type of test part used and the features the test part contained. Both systems measured the same test part.

The nature of milling makes each pocket of the test part to be slightly irregular. The inner walls of the pockets are slightly sloped, making the diameters of the pockets on one side of the test part slightly different from the diameters of the same pockets on the opposite side. This should only affect the MVS because it can only measure what is visible on the surface, while the CMM utilizes points along the surface and the interior of the pocket for measurement. The pockets of the test part are assumed to be circular.

The following list details the scope of the project. Specifics can be found in Chapter 3.

- Machine a test part that contains four circular pockets for measurement
    - Size of pockets: 0.5”, 1”, 1.5”, 2”
- Measure the test part on CMM and MVS
- Determine the appropriate formula to convert pixels to inches
- Determine the relevant accuracy of MVS using CMM as benchmark

The greatest difficulty in determining the accuracy of the MVS lies in the nature of the measurement data. The MVS outputs measurements in pixels. A mathematical equation must be used to convert the measurements from pixels to a suitable unit of measurement. Inches are used for this project. The equation is created by the operator, using the CMM measurements as a reference. The accuracy of this equation depends on the accuracy of the CMM measurements and the consistency of the MVS measurements. This equation is discussed in greater detail in Chapter 3, under the “Data gathering procedures” section.

CHAPTER TWO: LITERATURE REVIEW

BACKGROUND THEORY

The traditional metrology techniques require distances to be measured manually. This approach is "time consuming, prone to errors and invasive (Wang et al, 2002, p. 556)." The use of machine vision based metrology allows measurements to be taken with greater accuracy and efficiency.

There are some major advantages to machine vision based metrology. This approach is user friendly; the process is rapid, simple and minimally invasive; and the measurements are digitally stored for future use (Wang et al, 2005). One of the focuses of metrology in machine vision is to take 2D images and reconstruct them as a 3D model using geometrical entities. The techniques to do this are developing more and more every year.

The science of Machine Vision is still a relatively new field. This branch of study was formed from segments of several other branches of study. Among them are Physics, Artificial Intelligence, and Optics (Os et al, 2007). The following timeline is a brief history of Machine Vision, from the early stages to the present, and is compiled from the works of several authors (Köthe et al, 2005; SRI International, 2006).

1955: Selfridge publishes a paper in which he mentions "…eyes and ears for the computer"

1965: Roberts publishes “Machine Perception of Three-Dimensional Solids,” in which he demonstrates how a computer can produce a 3D model from a single 2D photograph.

1966-1972: Shakey the Robot – One of the first autonomous mobile robots. The first prototype used a mobile cart with a TV camera and an optical range finder, and was controlled from an SDS-40 over radio and TV links.

1975-1979: SRI Vision Module – A device for industrial part recognition using a trainable decision tree procedure.

1976: Image Understanding (IU) – Machine Vision Techniques are applied to photo interpretation as part of the ARPA IU Program.

1978: Machine Intelligence Corporation (MIC) founded – Charlie Rosen left SRI to start a company to manufacture and market vision models and, later, robot systems.

1979: Nagel publishes “Digitization and analysis of traffic scenes,” which incorporates natural scenes with motion.

1981: RANSAC (Random Sample Consensus) – Publication of a paper that introduced a new, now widely accepted paradigm for robust computation (and also presented the solution to some previously open problems in imaging geometry).

1982-1984: ImagCalc – An image analysis system that provided flexible access to 2D image processing tools, including displays at multiple resolutions, perspective projections, and a wide range of image operators. This was the

first interactive single-user image processing and manipulation system coupled with a high-resolution bit-mapped display.

1983: Image Understanding (IU) Testbed – SRI was chosen as the site of the ARPA IU Testbed, a facility that integrated much of the vision work supported by ARPA at that time.

1984-1986: TerrainCalc – An interactive system for synthesizing realistic sequences of perspective views of real-world terrain. TerrainCalc introduced the idea of the fly-through, created using texture-mapping aerial imagery onto digital terrain models.

1985: StereoSys – A hierarchical area-based matching system for the automatic construction of 3-D models from stereo pairs of images.

1986: Epipolar-Plane Image Analysis (EPI) System – A system that can effectively construct a 3D description of a scene from a sequence of images.

1996: Dicksmanns develops autonomous navigation on highways

2002: Bülthoff develops face modeling/recognition software

2003: Hongeng develops automated motion tracking and criminal act recognition

Studies over the past 300 years have been performed to explain our sense of color. Newton determined that color can be associated with frequency, but currently, there is no solid explanation as to what color is. Humans see color as tri-chromatic, and many Machine Vision Systems have been developed using tri-chromatic algorithms. A study performed in 2002 (Conklin et al) shows that dichromatic algorithms can be used to

successfully process color information. This simpler algorithm is faster and requires less expensive hardware to operate. The study concluded that the only drawback is the noise sensitivity experienced by the system, which can be countered by implementing additional sensors.

Ehrenman (2005) states that many factories are switching to vision-enabled robots so their robots can adapt to the ever-changing production environment. The robots without MVSs cannot adjust for changes that may take place mid-production (when a part has shifted) and can cause stoppages in production. These stoppages can be very costly to the company. Vision-enabled robots can see that a change has occurred and are able to compensate for it. MVSs are inexpensive, fast, and easy to use; the time and money a company can save by avoiding stoppages in production far outweigh the initial cost of a system. The cameras can be installed wherever they are needed, above the work cell or directly on the robot.

THEORY OF MVS OPERATION

There are several features that are critical for building a successful MVS. The system must be easy to use, available for a reasonable cost, operate in real-time, and provide reliable results. In addition to these requirements, most systems must be designed to operate independently of other systems. The design and development of a free-standing system often requires knowledge of a broad range of skills, such as lighting and

automation. Lighting is a crucial part of any successful machine vision system, and is discussed in detail in the “Lighting techniques and sources” section of this chapter.

The specific components that make up a MVS differ, but the same general requirements are the same. A MVS is composed of a camera, an image capture device, a lighting system, a computer, and software. The computer software converts the images into electronic signals and relays them from the image capture device to the computer, where they can be analyzed and stored. The type of analysis performed varies greatly; but, in general, the computer transforms the image into meaningful information.

The vast majority of image capture devices used today are charge-coupled devices (CCDs). When an image is being captured, the CCD simply detects the local light intensity that is projected onto the sensor. Current technology allows for the production of task-specific optical metrology devices, thanks to advancements in semiconductors. There are two variations of the typical CCD, Lock-In and Convolver. A Lock-In CCD works by measuring “local phase, amplitude and offset of a sinusoidal electrical signal (Spirig et al, 1995, p. 11).” A Convolver CCD works by shifting pixels bi-directionally and taking the summation of the original and the newly formed pixels. This method can also be used to capture multiple images of one subject over time for analyzing. “Each pixel has its own associated storage area, realized as an additive CCD column with separate gates in parallel to the main CCD column. (1995, p. 13).” Through the use of filters, this method has been implemented with a high degree of accuracy.

RELATED OR SUPPORTING THEORY

The most effective method for improving a procedure is to reduce or eliminate sources of variation. It is undeniable that "…variation exists in any production [or] service process, generally due to factors inherent in the design of the system, which cannot be easily controlled (Evans et al, 2005, p. 96)." Deming, a pioneer in the advancement of quality, stressed the importance of identifying and reducing sources of variation through improvements to design, technology, and training (Evans et al, 2005). Variation is identified and quantified through the use of statistical analysis, which provides a clear view of a situation, making it the ideal tool for improving a production or service process.

The Design of Experiments method is a statistical analysis tool that was developed in the 1920s by R.A. Fisher. The Englishman established the method to allow a comparison to be made between two or more methods to optimize yield or minimize variability within a process. In the process, levels of controllable factors can be determined and response variables can be examined for sources of variability. The DOE method can be applied to improve any process that contains a variable, and the number of samples required is substantially reduced due to the evaluation of discrete levels. "A paint company might be interested in determining whether different additives have an effect on the drying time of paint in order to select the additive that results in the shortest drying time (Evans et al, 2005, p. 542)."

Another way to improve a production or service process is through the use of continuous measurement. Continuous measurement provides more information for the same sample

size over pass/fail, or a smaller sample size can be used to acquire the same amount of information. A study done in 2002 by Michael Hamada found that continuous data provided 5.4% greater confidence level over pass/fail data with a sample size of 20, and 8.7% with a sample size of 25. Furthermore, the study found that a sample size of 75 is required for pass/fail data to achieve the same confidence level obtained from continuous data gathered from a sample size of 10 (Hamada, 2002).

RESEARCH RELATING TO APPLICATIONS

MVSs can identify size, shape, color, and texture of objects as well as provide numerical data to represent the characteristics of each object. These systems are noted as being accurate, nondestructive, and consistent. The camera-based systems are known for their simplicity, low cost, rapid inspection rate, and versatility. Most monochrome systems (such as the one used in this study) are able to capture objects in visible color (VIS) and near-infrared (NIR). One of the applications for MVSs is agriculture. As it was pointed out in an article from *Computers and Electronics in Agriculture* in 2002 (Chen et al), advancements in MVSs have made them faster, allowing them to meet the real-time speeds needed in agricultural processing centers. Some examples of its use in agricultural applications include: “automatic segmentation of the rib-eye area from a cut surface of longissimus muscle and for the determination of the degree of marbling in the beef rib-eye area (2002, ¶ 14);” the “detection of blemishes and bruises on apples (2002, ¶ 14);” and “detecting scars, cracks, and spreading tips for asparagus (2002, ¶ 14).” This technology can increase productivity while reducing cost. MVSs also create a safer work

environment for employees while producing a safer and higher quality item for consumption.

The following is a brief list of typical applications of MVSs, taken from a presentation given by U. Köthe (2005):

Industrial Image Processing:

Process control, quality control, geometrical measurements

Robotics:

Assembly, navigation, cooperation, autonomous systems

Monitoring:

Event recognition, safety systems, data collection, smart homes

Aerial image analysis:

GIS applications, ecological issues, defense

Document analysis:

Handwritten character, layout, and graphics recognition

Medical image analysis:

Image enhancement, image registration, surgical support

Image retrieval:

Image databases, multimodal information systems, web-info retrieval

Virtual reality:

Image generation, model construction

Creating custom prosthetics/orthotics from digitized human body surfaces (Bhatia et al). “A 3D optical range sensing scanning system that can detect and

locate virtually the entire surface of a complex object in less than one second… (1991, p. 925)."

Obtaining measurements from crime scenes through the use of "reference lengths…measured from fixtures such as tables and windows (Criminisi et al, 1999, p. 25)."

Creating a 3D model of 2D paintings by "recovering sets of parallel planes and directions (Criminisi et al, 1999, p. 26)."

Notifying operators when a piece of equipment requires cleaning or maintenance by monitoring the tolerance limits of a production process (Pastorius, 1988).

In 1994, Rontang Ling developed a two-stage technique for 3D camera calibration for machine vision based metrology. The first step computes the camera's pose in the *x* and *y* axes. The second step computes the camera's focal length (effective), distortion coefficient, and *z* position. These simple steps can be applied to most any camera type. Another IEEE study, from 2006 (Renaud et al), discusses the use of various digital cameras for 3D measurement. The cameras calibration is vital to accurately calculate 3D coordinates/pose of an object, and a calibration target or artifact is usually required for accurate calibration. However, the study proves that "camera calibration no longer requires an accurate calibration target (2006, p. 13)." The study goes on to show that vision-based metrology can be implemented as a tool to calibrate parallel mechanisms, like Stewart platforms.

In 2008, a study was published by IEEE (Mendonça et al) detailing how a single-view MVS can "accurately measure the angle of compressor stator vanes in jet engines…and can replace expensive, custom-made, hard gauges which are currently used to measure the stator vanes (2008, p. 1)." The system utilized a mapping system to define the metrics needed for accurate measurement.

Another study shows how a MVS can be used to solve problems surrounding machining tool wear measurement (Jurkovic et al, 2005). When used in conjunction with a laser diode, with a linear projector, a MVS can create a 3D image of an object without the need for complicated and expensive measuring equipment. These systems are simple, robust, flexible, and cost-effective. The two factors that limit a tool's life are flank and crater wear. These are usually examined manually under a microscope, but the process is inaccurate and time consuming. Using direct optical measurement, the wear patterns can be accurately examined. The only setback is the difficulty lighting the tool, creating an issue with automating the process. The flank wear can be easily examined using a MVS, but the crater wear must be examined using a different method. For the flank measurement, the texture of the tool is represented by changes in the grey level of the tool. A mathematical formula is used to change the grey distribution into a 2D histogram that follows the contour of the tool surface. Projected laser lines must be incorporated to allow crater depth to be measured. The angular properties and deflection of the light (laser) correspond directly to the 3D dimensions of the tool. This process can be fully automated, and in the future, 3D profiles could be generated using the same laser line angle method.

These studies show that the MVS is a proven tool for identifying the size and shape of objects and is noted for its accuracy and consistency. The MVS is also celebrated for its simplicity, low cost, rapid inspection rate, and versatility. MVS technology helps increase productivity while reducing cost. The single-view type MVS used in this study has been proven to accurately measure complex geometries without the need for a calibration target. In fact, the MVS can be used to calibrate other mechanisms. The difficulty of lighting the target is the only drawback to the MVS.

COMMON METHODS OF MEASUREMENT/ANALYSIS OF DATA

A good method for identifying and controlling variation within a measuring system is the six sigma tool known as GR&R, which stands for gage repeatability and reproducibility. This tool measures the amount of variation in the measuring system that arises from the measurement device and the people taking the measurements. Through the regular use of this tool, variability associated with measurements and the measuring device can be identified and corrected. It is important to note that this tool alone cannot catch all sources of variation in a system. Edward P. Morse found that **"**…a "golden" part with good geometric characteristics (minimal within-part variation) and "known" values…used in conjunction with the GR&R study, [will show] the difference (if any) in the variability between the average part and the golden part (2002, p. 3)."

Another method, outlined by W. J. Pastorius in his 1988 study of *Machine Vision for Industrial Inspection Metrology and Guidance*, suggests the use of a "silver" master to

aide in regular calibration. The study suggests taking a regular part from the production line, sending it to a CMM, and digitizing the part. The digital data, along with the physical part, are then used as a calibration target/artifact for the MVS, since the digital data contains the actual measurements to use as a reference. This method allows the MVS to calibrate itself.

A study to improve defect detection in apples using a MVS was performed in 2004 (Bennedsen et al, 2005). The study's goal was to improve the system's ability to distinguish between defects and false positives, which are caused by shadows created by the surface characteristics of the object (apples in this case). One approach implemented new lighting techniques but still experienced false positives at a rate of 1.1-3.6%. Even though consumers associate the quality of the outer surface with the quality of the fruit itself, and companies want to eliminate all unsatisfactory fruit, they do not want to eliminate any good fruit, especially when the loss would be caused by insufficient sorting equipment.

The method used by the MVS in this study rotates the apple 360° and captures six images during rotation. The images are eight-bit grey scale and are filtered through a 740 and 950 nm filter, producing twelve images. The 740 nm filter creates dark spots for diseases, while the 950 nm filter creates dark spots for bruises. As the conveyor rotates the apples, the shadows change position, but the defects (dark spots created by the filters) stay in the same area. The speed of the conveyor allows for the same area of the apple to be captured multiple times, and if the dark spots can be seen in three or more consecutive frames,

then it is most likely a defect. In this study, the conveyor rotated the apple 30°, causing defects to sometimes be visible in only one frame. Preferably defects would appear in three to six frames.

The study examined two different types of apples, Pink Lady and Ginger Gold. After capturing the images on the conveyor, both the 740 and 950 nm filtered images were combined for evaluation. Images with a defect were given a value of 1 while images with none were given a value of 0. The values of the images were summed, and apples having a value of 3 or greater were considered defective, while those of 2 or less were considered to be fine. The system successfully detected 92% of the defects in the Pink Lady batch with only one false positive and detected 90% of the defects in the Ginger Gold with no false positives. Improvements could be made by increasing the number of images captured of each apple and/or by increasing the number of cameras used to capture the images.

RELEVANT STATISTICAL PROCEDURES

The method to calculate accuracy is simple. The variance of the data gathered from the MVS is computed and evaluated for each data set individually, the lower the variance, the greater the accuracy. The limiting factor is the equation used to convert data from pixels to standard dimensions, which is completely reliant on accurate measurements from both the CMM and the MVS. When the dimensions of the target object are known the CMM data is easily verified.

In order to fully evaluate the accuracy, an acceptable amount of error must be established. The following formulae are taken from a quality textbook (Evans et al) and are considered to be the standard formulas to use. The acceptable amount of error can be represented as a function of: (ε_T) For the sake of the following example, assume $(\varepsilon_T = 0.7)$. The next step is to establish a null and an alternative hypothesis.

$$H_0^A : \mu_\varepsilon = \varepsilon_T \qquad H_1^A : \mu_\varepsilon < \varepsilon_T$$

A *t*-test is performed to evaluate these hypotheses. The following equation is a *t*-statistic:

$$T_0 = \frac{\overline{X} - \varepsilon_T}{S/\sqrt{N}}$$

The *t*-values obtained from the *t*-test determine whether a hypothesis is accepted or rejected. The rejection or acceptance of the null hypothesis or the alternative hypothesis is made at a significance level equal to α, usually 0.05. This means that the decision is made with a 95% probability that it is the correct conclusion.

Failing to reject the null hypothesis does not imply that the error is 0.7, but that the error is definitely not (with a 95% confidence level) less than 0.7. An alternative hypothesis is needed to show an unacceptable amount of error:

$$H_1^{'} : \mu_\varepsilon > \varepsilon_T$$

LIGHTING TECHNIQUES AND SOURCES

The goal of lighting in machine vision is to illuminate the target object so that the camera can obtain the best image possible. The image should have a high contrast between the features of the target object and the background. This is done by separating the target object from the background utilizing four optical properties of the object: shape, translucency, texture, and color. The lighting should be controlled and consistent, so that the machine vision system obtains consistent and reliable images for analysis.

There are three basic lighting techniques to choose from: front, back, and structured.

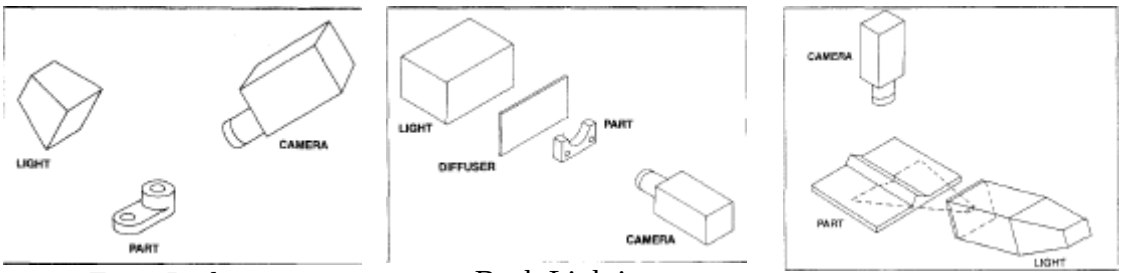

Front Lighting Back Lighting Structured Lighting

Figure 2 – Lighting Techniques
(Novini, 1993)

- Front Lighting requires that the camera and the light source be on the same side of the object plane. The angle of the camera and light source to the target depends on the effect the user is after. Front lighting is primarily used for surface inspection. It is also the preferred method for monochrome applications.

- Back Lighting requires that the camera and the light source be on opposite sides of the object plane. The camera and the light source are usually perpendicular to the

target, but this is not a requirement. This technique provides the most contrast, but only provides silhouette information.

- Structured Lighting is a light source with some mechanical means of controlling the shape and form of the projected light. This can be done with apertures, lenses, and lasers. In Figure 2, a slit has been cut in a light box to create a narrow line of light. Structured lighting has many applications, many of which fall into two categories: limiting the light projected to reduce the complexity of the scene, and obtaining three-dimensional data using a two-dimensional system.

The angle of the lighting source creates two different lighting effects: bright field and dark field. The area perpendicular to the part (in front or behind), and the area slightly askew of this area, is known as the bright field. The area parallel to the part (in front or behind), and the area slightly askew of this area, is known as the dark field. An illustration indicating the location of these fields can be found in Appendix A. The quality of the light also needs to be considered when choosing the appropriate lighting angle. The two levels of light quality are diffuse and collimated.

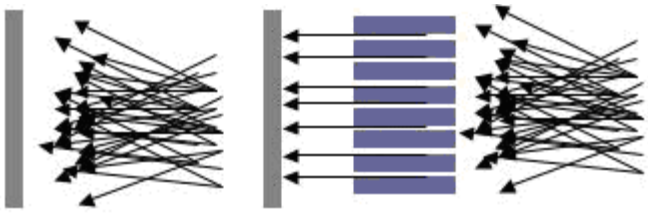

Figure 3 – Diffuse and Collimated light (Verdon, 2004)

In Figure 3, the example on the left resembles diffuse light, while the right resembles collimated light. Usually, when dealing with high-speed camera systems, diffuse light requires 10-100 times the power as collimated lighting to achieve the same effect. However this is not true in all cases. Whenever the surface of the target object is shiny or reflective, diffuse light is the best choice. Any irregularity in the surface of the target object may require the light source to be moved closer to the target object. The use of collimated lighting is a must for most backlighting operations, because it helps prevents the light from wrapping around the target object, which can cause the edges to become blurry. Collimated light is also useful for surface defect detection through bright-field front-lighting.

There are several factors to consider when choosing the appropriate light source for a machine vision system. The lighting technique, and type of analysis being performed, has a big influence on the light source used. The properties of the target object are equally important. The cost and expected life span of the light source also factor into the equation. In some cases the cost is much greater for only a minor improvement in performance. The safety of the operator and of the equipment must also be taken into consideration. Harmful radiation or high-heat output may require special shielding be put in place.

There are seven basic illumination sources to choose from: Incandescent, Fluorescent, Xenon, LED, Infrared, Ultraviolet, and X-ray.

- Incandescent or filament bulbs have a high level of light output that is generated through resistance. This resistance is created by passing electricity through a filament, and causes a large amount of heat to be discharged from the light source. Some common incandescent bulbs include tungsten (household bulb) and halogen. A benefit to using incandescent lighting is the smoothing of the 60Hz ripple, which is discussed later. These bulbs are inexpensive and have varying life expectancies.

- Fluorescent lamps generate light by exciting electrons (through an inert atmosphere) with an electrical arc. This process generates a large amount of ripple. These lamps discharge a comparably minute amount of heat, and require very little power compared to the illumination provided.

- Xenon flash tubes are used for strobe lighting. The quick flash of light, when timed right, makes objects on a high-speed conveyor appear to be still, allowing them to be analyzed with greater ease. A xenon light source provides high power over a wide spectrum. The only challenge is ensuring the light and the camera are in sync.

- LED or light-emitting diode is “a PN Junction diode which emits light when biased in a forward direction (Novini, 1993).” A PN Junction diode is composed of p-type and n-type semiconductors, making the LED a solid-state semi-conductor light source. The typical LED has a life expectancy of 30000-100000 hours, low power consumption, and low heat output. The small size of the LED requires the use of many to light an object. Although this can be expensive, the cost is falling as the

technology advances, and the performance is rising. The small size also allows the LED to be placed in configurations that would be impossible for other light sources.

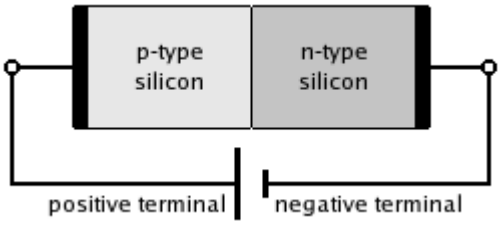

Figure 4 – Forward bias PN Junction (Ramadan, 2006)

- Infrared (IR) radiation has a wavelength that is longer than that of visible light. Many cameras that are used in machine vision can see into this spectrum of light. These light sources are considered to be one of the most efficient in terms of power use.

- Ultraviolet (UV) light has a wavelength that is shorter than that of visible light. The shorter wavelength makes it the most useful for inspections at the smallest scales (around 500nm (Vickers, 2009)). UV light can also make transparent objects, that do not transmit UV, opaque; which allows them to be measured with less complexity. In many manufacturing settings, UV sensitive ink is used to mark various items of interest on objects. These items can vary from tracking numbers to defects.

- X-ray (x-radiation) has a wavelength even shorter than UV light. X-rays are a nondestructive method for inspecting objects for internal flaws. The radiation penetrates objects, creating an image of the interior. These images used to be captured on film and then analyzed by an operator; this was true for medical and

industrial applications. The downside was the high amount of error caused by poor imaging and interpretation. With advances in digital image processing, machine vision systems are now used to capture and analyze these images.

A word on “Ripple”: According to an FAQ from Edmund Optics, “‘Ripple’ is a sinusoidal fluctuation of light intensity (Edmund, 2009).” The fluctuating light intensity affects the accuracy of measurements gathered by a machine vision system. For a machine vision system to work properly, the light source must provide consistent illumination of the target object. The ripple effect is caused by the fluctuation of power associated with using an AC power source. Ripple is also known as 60-cycle hum and light drift.

The fluctuation in light sources is usually not visible to the naked eye, because the flicker is so rapid, but it is easily detected by high-speed cameras. Sometimes the flicker can be observed in fluorescent tube lighting that is damaged or at the end of its life cycle. Although some experts and companies claim to “fix” the problem using line, current, and/or voltage regulation, the only real solution is to switch to a DC power source.

CHAPTER THREE: METHODOLOGY

PRELIMINARY PROCEDURES

A test project was performed to better understand how to develop an effective inspection procedure for visual analysis of dimensional data for selected part geometries. The initial program utilized the Pattern Sort inspection tool, and the results of the experiments performed using these methods have been used to develop an improved method of data collection. The first issue that arose was lighting. The fluorescent lighting found in the laboratory caused interference with the image capturing capabilities of the camera. A fixture to block the fluorescent lighting was implemented, and a halogen light with 500 watts of power illuminated the target object. The original placement of the camera for the initial test project also established the need for a permanent camera jig. The permanent jig allowed for constant camera settings and aids with the lighting issue.

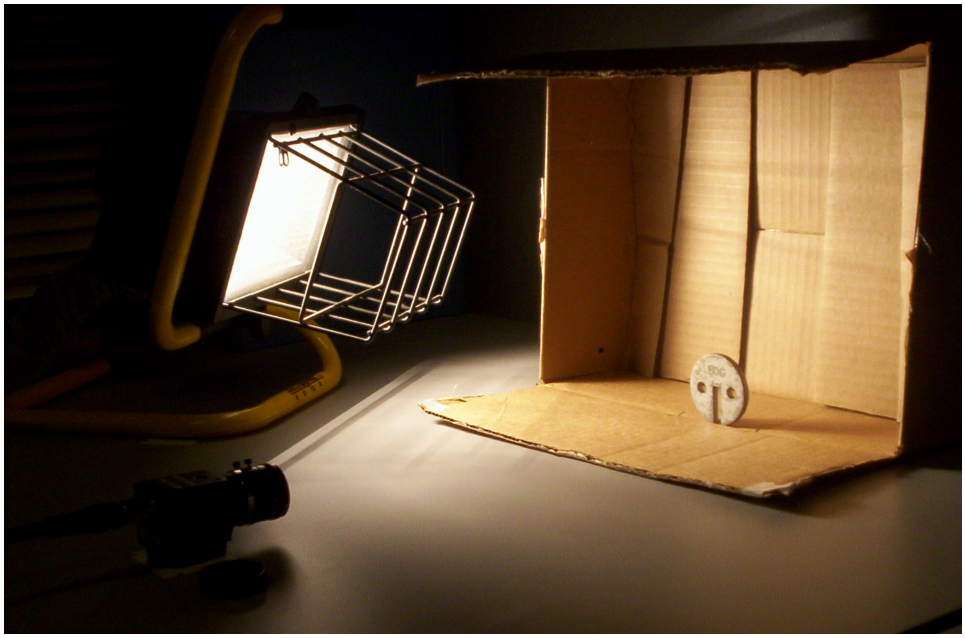

Figure 5 – Improvised Test Setup

Figure 6 – Improved Test Setup

Through the use of the permanent jig, another experiment was conducted to determine the best lighting setup. This experiment utilized the Edge Width inspection tool to measure the width of a gage block of known dimensions. The only variable that was changed was the type of bulb used for the lighting. The goal was to determine if different bulbs produced different amounts of variation in the measurement data. The full details of the experiment can be found in the Data Gathering Procedures section.

EXPERIMENTAL DESIGN

The following experimental design (Diamond, 1989) is used when analyzing differences in population mean when variance is unknown. This experimental design was chosen because it has not only been verified by statisticians, but by industry as well. For this experiment our number of iterations needed (N) can be calculated by defining a few variables (α, β, and δ) and using a probability table. The risk of making a Type I error (rejecting a good part) is represented by α. The risk of making a Type II error (accepting a bad part) is represented by β. The difference between the two means being evaluated is represented by δ. Since the variance is unknown, δ is specified in terms of σ.

$$H_0 : \mu_1 = \mu_0 \qquad \alpha = 0.05 \qquad \beta = 0.10 \qquad \delta = 0.5\sigma$$

$$N = (U_\alpha + U_\beta)^2 \frac{\sigma^2}{(\delta)^2} = (1.645 + 1.282)^2 \frac{\sigma^2}{(0.5\sigma)^2} = 34.27$$

Since the *t* distribution is being used, instead of the normal distribution, another formula must be used. Again, a probability table is necessary.

$$\phi = N - 1 = 33.27$$

$$N_t = (t_\alpha + t_\beta)^2 \frac{\sigma^2}{\delta^2} = (1.70 + 1.31)^2 \frac{\sigma^2}{(0.5\sigma)^2} = 36.48$$

This result means that a minimal acceptable sample size is 37. A sample size of 50 will be used to compensate for any unforeseen problems.

DATA GATHERING PROCEDURES

The ability of a vision system to accurately measure or analyze anything relies heavily on having the right light source. A preliminary experiment tested three different light sources; two incandescent or filament bulbs (Tungsten and Halogen), and one fluorescent or discharge lamp. The variation in wavelength is a contributor to ripple observed. A company has measured the residual ripple from systems using 60-cycle power as: Fluorescent = 60%, Tungsten = 10%, Halogen ≤ 10% (Mercron, 2008).

The camera jig used for this experiment was designed for overhead inspection of parts on a conveyor. The camera was positioned perpendicular to the target object. The light sensor was attached to the camera so that it reads the light reflected from the target object at the same location the camera is capturing images. A thermometer was also attached to the camera. The temperature was monitored to ensure the camera was not being harmed. The camera should not be operated in environments above 122°F. Two clamp lights were attached on each side of the camera. These lights were positioned to provide front, bright-field, diffuse illumination. The lights feature a 10.5” aluminum reflector, an Edison socket, and 250watt maximum capacity (each).

The data was gathered using Logger Lite software and a LS-BTA Light Sensor, both from Vernier Software & Technology. The following table is a summary of the data before analysis.

Bulb #	Type	Brand	Power	Lumen Rating	Start Temp	Stop Temp	Max Lux	Median
			watts	lm	°F	°F	lux	lux
1	Fluorescent	Sylvania	40**	2600	80	89	2040	1911.2
2	Tungsten	Sylvania	150	2740	82	100	2465	2417.5
3	Halogen	GE	150	2430	82	96	2119	2027.0

**The fluorescent bulb, although 40 watts, is considered the 150 watt equivalent.

Table 1 – Summary of Raw Bulb Data

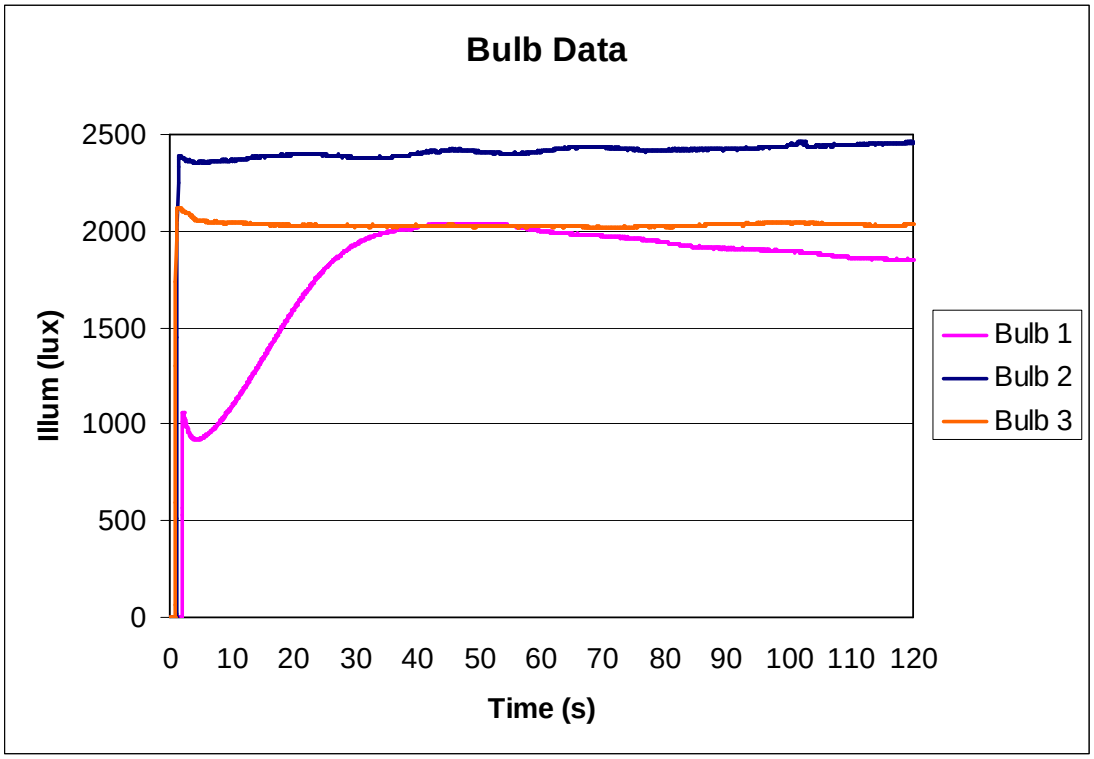

Figure 7 – Bulb Data

The test was initiated with the light fixture turned off. Once data collection began, the light fixture was turned on. This was done to determine if any of the bulbs required a period of time to “warm-up” in order to reach their full brightness. It is easy to see that

the fluorescent bulb (Bulb 1) needed this warm-up period. This bulb was eliminated, since the bulb with the least amount of variation is desired. The remaining bulbs required more evaluation to determine which bulb is the better choice. In order to gather data better suited for statistical analysis, another experiment was conducted. For this experiment the camera and light fixtures remained in the same positions as before, and the Keyence MVS was used to gather measurement data.

A program was written for the MVS to measure the width of detected edges. A calibrated gage block (0.400”) was used as the target object. The tungsten bulbs were placed in the light fixtures and the program was run for 50 iterations. The tungsten bulbs were then replaced with the halogen bulbs, and the program was run for 50 iterations. All data, including tables and graphs, can be found in the original report.

The data was converted from pixels to inches by dividing the known width of the target object (0.400”) by the average of all pixel measurements for each set of data. The result was the “conversion factor” that can be used to convert pixels to inches and visa versa. The conversion factors are as follows:

Tungsten:	0.005286
Halogen:	0.00532

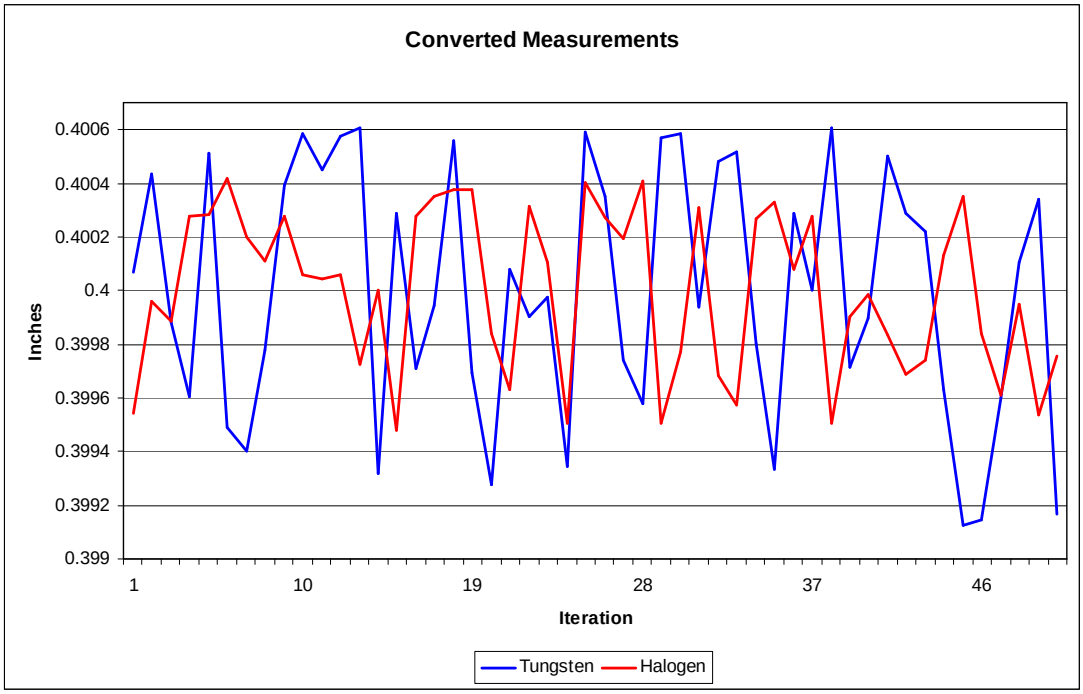

Figure 8 – Converted Bulb Measurements

The first step in analyzing the data was to determine the appropriate tests to conduct and the hypotheses to go along with them. The data is continuous, assumed to be normally distributed, and contains two samples. Therefore an F-Test was performed. The null and alternative hypotheses are as follows:

$$H_o : \sigma_1 = \sigma_2 \qquad H_a : \sigma_1 \neq \sigma_2$$

The results of this test are as follows:

F-Test Two-Sample for Variances

	Tungsten	*Halogen*
Mean	0.4	0.4
Variance	2.17033E-07	9.11239E-08
Observations	50	50
df	49	49
F	2.381737184	
P(F<=f) one-tail	0.001456953	
F Critical one-tail	1.607289464	

Table 2 – F-Test Results for Bulb Data

The p-value shows that there is a 99.85% chance that the results of this test are statistically significant. The F-ratio is greater than the F-critical, which means there is a statistically significant difference between sample variances. For these reasons the null hypothesis is rejected. The results of the F-Test are graphically illustrated in Figure 9.

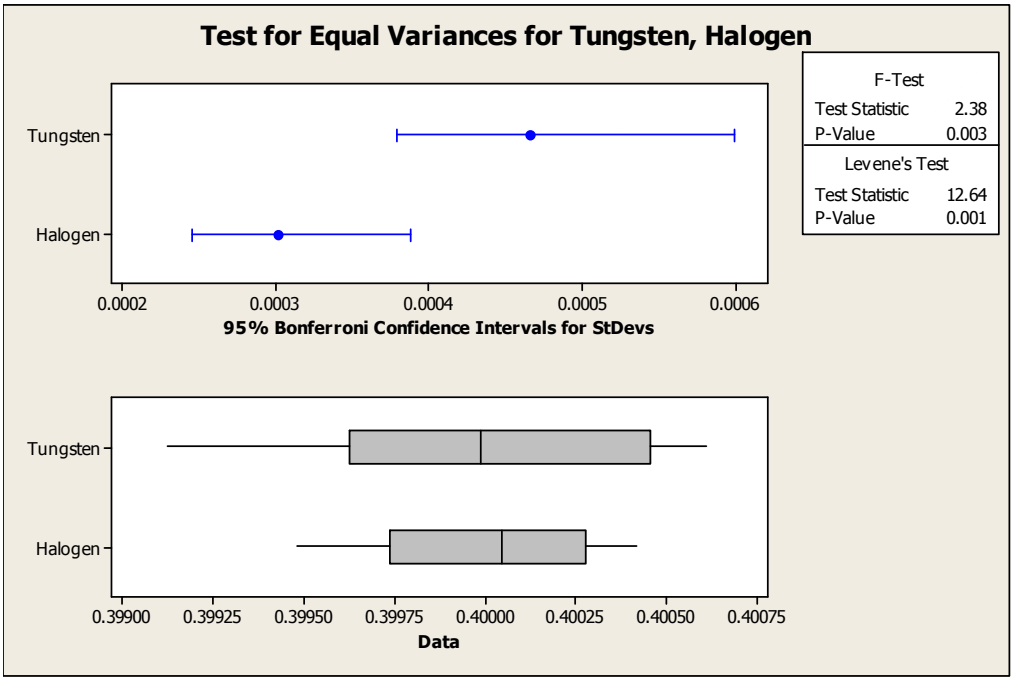

Figure 9 – Test for Equal Variance for Tungsten & Halogen

The data was determined to have unequal variance, so a Two Sample t-Test assuming Unequal Variance was performed. The results of this test are as follows:

t-Test: Two-Sample Assuming Unequal Variances

	Tungsten	*Halogen*
Mean	0.4	0.4
Variance	2.17033E-07	9.11239E-08
Observations	50	50
Hyp. Mean Diff.	0	
df	84	
t Stat	0	
P(T<=t) one-tail	0.5	
t Critical one-tail	1.66319668	
P(T<=t) two-tail	1	
t Critical two-tail	1.988609629	

Table 3 – t-Test Results for Bulb Data

The problem with these results is that a t-Test examines the difference between two means, and the means of these two groups are equal (0.400”). Therefore, in order to determine the best bulb to use, the variance of each bulb was compared. The halogen bulb has the lowest variance and therefore is the better choice for lighting.

In addition to the corrections made as a result of these preliminary experiments, other items needed to be addressed before meaningful data could be collected. Primarily, a test part was required with which to perform the tests. The test part was machined in order to highlight various features for measurement. These features include four circular pockets of varying size, as shown on the following page.

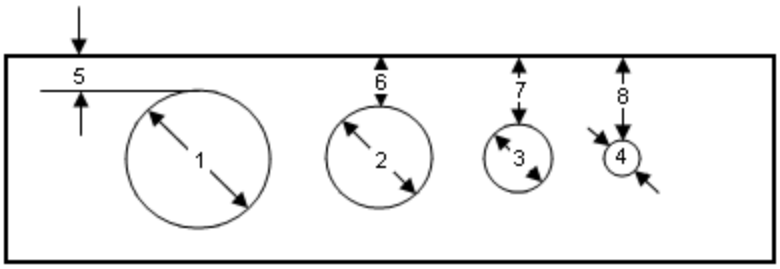

Figure 1 – Test Part

The next step was to develop Edge Width inspection programs, using the Keyence MVS, for various feature measurement. The test part features required that two Edge Width programs be implemented; one that measures Inner Gap and one that measures Outer Gap. The test part was measured 50 times for each feature with both the CMM and the MVS. The gathered data was then used to solve for the missing variable (φ) in the formula found below.

$$\overline{X}_{MVS} * \varphi = \overline{X}_{CMM}$$

After solving for φ, the following formula is used to convert the MVS measurements from pixels to inches.

$$X_i(pixels) * \varphi = X_i(inches)$$

After converting all the data, the accuracy of the MVS measurements were then evaluated using the CMM measurements as the assumed correct data.

MEASUREMENT METHODS AND PROCEDURES

The vision system being used is a Keyence CV-3002 Series: Multi-camera Universal Machine Vision System, with a CV-035M Series: Double Speed Digital Camera (Monochrome). A list of features for these two components can be found in Appendix A. The CMM being used is a Zeiss Contura G2 (HTG) (High Temperature Gradient). This is a bridge-type CMM with an accuracy of ± 2µm.

The test part was measured using both the Keyence MVS and the Zeiss CMM. The Keyence system utilizes the Edge Width inspection tool. Once the data was collected, an analysis of the Keyence system's accuracy was performed, using the Zeiss measurements as the standard.

PROCEDURES FOR ANALYZING DATA

The conversion of the MVS data from pixels to inches created a problem when analyzing the data. The conversion factor was determined by using the means of both the CMM and the MVS data, causing the mean of the converted data to be equal to the mean of the CMM data. With equal means, the only relevant statistical analysis available is an F-Test. The actual measurements are presented in Chapter 4.

CHAPTER FOUR: RESULTS

The CMM data was gathered first. A basic program was written in Calypso so that the measurement process was fully automated. The CMM measured the entire part at one time, obtaining one measurement for each feature each time the program was run. A full description of how the program was developed can be found in Appendix B. The average read time of the program was 5 minutes and 27 seconds. This is irrelevant, however, because the program was not written for speed. The probe was limited to 30mm/s and a large clearance plane was used to ensure there were no crashes. With minor programming changes and an increase in probe speed, the read time can be greatly reduced.

The test part was removed from the CMM platform and then put back after each run. This was done to replicate real world settings of unloading and loading parts for measurement, to verify if changing the parts orientation slightly would effect the measurements. The small number of points sampled by the CMM causes the location of these points to differ slightly each time the program is run. The HAAS milling machine used to create the test part is only capable of +/-0.0002” accuracy/repeatability, which only applies when the machine is set to “stepper” mode. A deviation of this amount, or greater, was expected because the machine was not in this mode when the test part was milled.

The MVS data was gathered next. The holes were measured first, using the Edge Width program written to measure Inner Gap. The widths were measured next, using the Edge Width program written to measure Outer Gap. The material used to construct the test part, black ABS plastic, proved to be a poor choice, as it became extremely hot under the

bright lights. The heating of the part meant that the dimensions were changing as the part expanded. In order to compensate for this, the part was left under the lights for 5 minutes before measuring each feature, so that any changes to the parts dimension would be minimal once data collection began. This method worked well until the part began to melt as the last measurements were being recorded.

The graphs and tables of the data before analysis follow. The tables include: raw data for the CMM and MVS, the mean of each group, the pixel to inches conversion factor, and converted data. The CMM* data in the Width tables represents the corrected width measurement. The details of how these measurements were obtained can be found in Appendix B. The statistical analyses of the data are presented in Chapter 5.

Mean	Mean	Convert			
2.0223	399.3523	0.005064			
		Hole #1			
CMM	Raw	Converted	CMM	Raw	Converted
2.022241	399.14	2.021115	2.022337	399.488	2.022877
2.022287	399.51	2.022988	2.02234	399.516	2.023019
2.02229	399.407	2.022467	2.022354	399.243	2.021636
2.022265	399.112	2.020973	2.02235	399.247	2.021656
2.022244	399.484	2.022856	2.022354	399.57	2.023292
2.02226	399.529	2.023084	2.022355	399.192	2.021378
2.022308	399.253	2.021687	2.022356	399.31	2.021975
2.022314	399.495	2.022912	2.022353	399.315	2.022001
2.022306	399.288	2.021864	2.02236	399.234	2.021591
2.022305	399.393	2.022396	2.022358	399.363	2.022244
2.022313	399.555	2.023216	2.022357	399.271	2.021778
2.022316	399.129	2.021059	2.022356	399.555	2.023216
2.022317	399.149	2.02116	2.02236	399.302	2.021935
2.022328	399.257	2.021707	2.022353	399.28	2.021823
2.022319	399.273	2.021788	2.022351	399.504	2.022958
2.022322	399.483	2.022851	2.022352	399.571	2.023297
2.0223	399.526	2.023069	2.022354	399.573	2.023307
2.022304	399.403	2.022446	2.022354	399.261	2.021727
2.022309	399.247	2.021656	2.022361	399.551	2.023196
2.022305	399.224	2.02154	2.02236	399.409	2.022477
2.022315	399.38	2.02233	2.022362	399.276	2.021803
2.022313	399.369	2.022274	2.022363	399.569	2.023287
2.022307	399.392	2.022391	2.022364	399.362	2.022239
2.022312	399.424	2.022553	2.022368	399.567	2.023277
2.022309	399.386	2.02236	2.022373	399.648	2.023687

Table 4 – Hole #1 Data

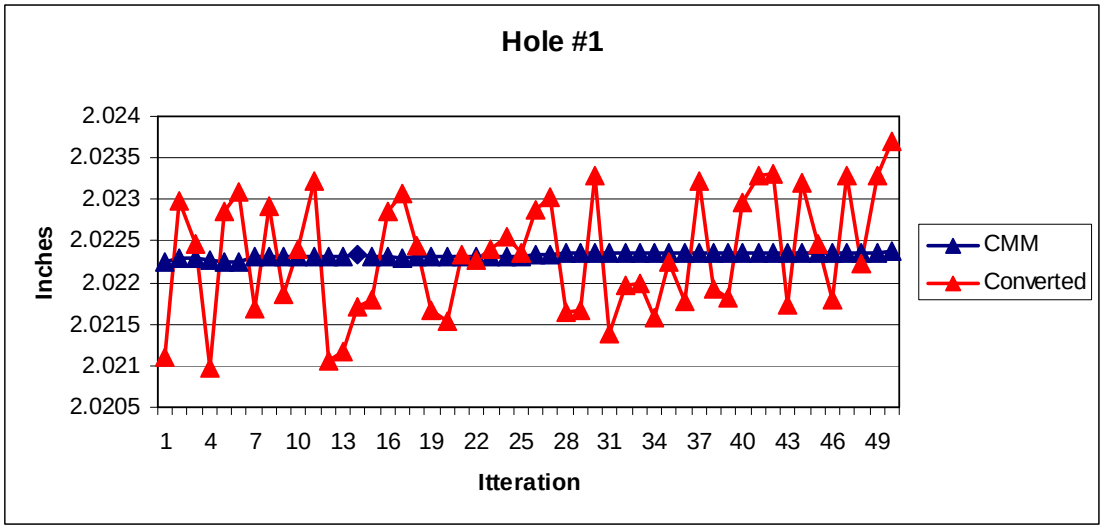

Figure 10 – Hole #1 Data

Mean	Mean	Convert			
1.521946	301.7598	0.005044			
		Hole #2			
CMM	Raw	Converted	CMM	Raw	Converted
1.521901	301.664	1.521451	1.52197	301.896	1.522621
1.521926	301.719	1.521728	1.521974	301.636	1.52131
1.52192	301.737	1.521819	1.521981	301.65	1.52138
1.521915	301.669	1.521476	1.521979	301.767	1.52197
1.521952	301.782	1.522046	1.521977	301.725	1.521759
1.52195	301.784	1.522056	1.52198	301.675	1.521506
1.521948	301.851	1.522394	1.521981	301.84	1.522339
1.52195	301.794	1.522107	1.521981	301.862	1.522449
1.521955	301.684	1.521552	1.521979	301.556	1.520906
1.521955	301.756	1.521915	1.521981	301.575	1.521002
1.52196	301.696	1.521612	1.521984	301.674	1.521501
1.521955	301.814	1.522207	1.521985	301.755	1.52191
1.521955	301.801	1.522142	1.521981	301.714	1.521703
1.521963	301.83	1.522288	1.521977	301.806	1.522167
1.521955	301.729	1.521779	1.52198	301.883	1.522555
1.521955	301.737	1.521819	1.521981	301.834	1.522308
1.521945	301.705	1.521658	1.521982	301.921	1.522747
1.521947	301.761	1.52194	1.521982	301.717	1.521718
1.521947	301.68	1.521532	1.521986	301.872	1.5225
1.521949	301.831	1.522293	1.521986	301.751	1.52189
1.52195	301.846	1.522369	1.521987	301.838	1.522328
1.521952	301.882	1.52255	1.521985	301.707	1.521668
1.521951	301.88	1.52254	1.521989	301.935	1.522818
1.521946	301.596	1.521108	1.52199	301.812	1.522197
1.521948	301.768	1.521975	1.52199	301.89	1.522591

Table 5 – Hole #2 Data

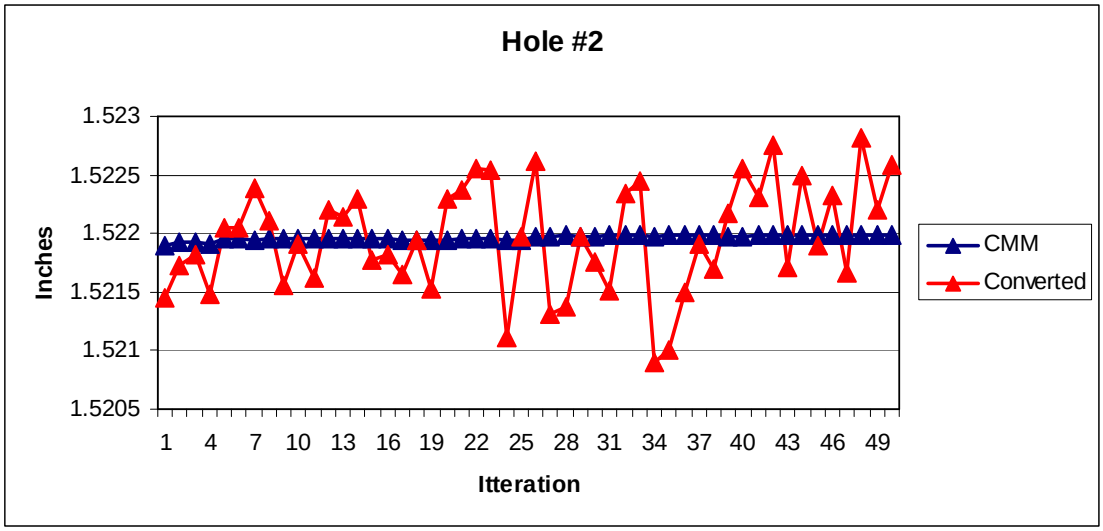

Figure 11 – Hole #2 Data

Mean	Mean	Convert			
1.020878	201.4788	0.005067			
		Hole #3			
CMM	Raw	Converted	CMM	Raw	Converted
1.0208	201.402	1.020363	1.020908	201.52	1.020961
1.020796	201.522	1.020971	1.020908	201.438	1.020545
1.020804	201.428	1.020495	1.020916	201.632	1.021528
1.020804	201.433	1.02052	1.020911	201.406	1.020383
1.020886	201.448	1.020596	1.020911	201.45	1.020606
1.020892	201.406	1.020383	1.020912	201.549	1.021108
1.02089	201.397	1.020338	1.020914	201.456	1.020637
1.020891	201.665	1.021696	1.020914	201.558	1.021153
1.020894	201.362	1.02016	1.020916	201.614	1.021437
1.020893	201.488	1.020799	1.020915	201.678	1.021761
1.020897	201.392	1.020312	1.020917	201.577	1.02125
1.020893	201.348	1.02009	1.020917	201.513	1.020925
1.020897	201.415	1.020429	1.020916	201.404	1.020373
1.0209	201.416	1.020434	1.020914	201.742	1.022086
1.020895	201.471	1.020713	1.020914	201.628	1.021508
1.020895	201.58	1.021265	1.020913	201.364	1.020171
1.020891	201.306	1.019877	1.020916	201.528	1.021001
1.020893	201.637	1.021554	1.020914	201.652	1.02163
1.020893	201.624	1.021488	1.020913	201.459	1.020652
1.020893	201.577	1.02125	1.020915	201.645	1.021594
1.020893	201.487	1.020794	1.020917	201.594	1.021336
1.020894	201.344	1.020069	1.020918	201.387	1.020287
1.020894	201.68	1.021772	1.02092	201.592	1.021326
1.020891	201.466	1.020687	1.020918	201.446	1.020586
1.020891	201.676	1.021751	1.020919	201.562	1.021174

Table 6 – Hole #3 Data

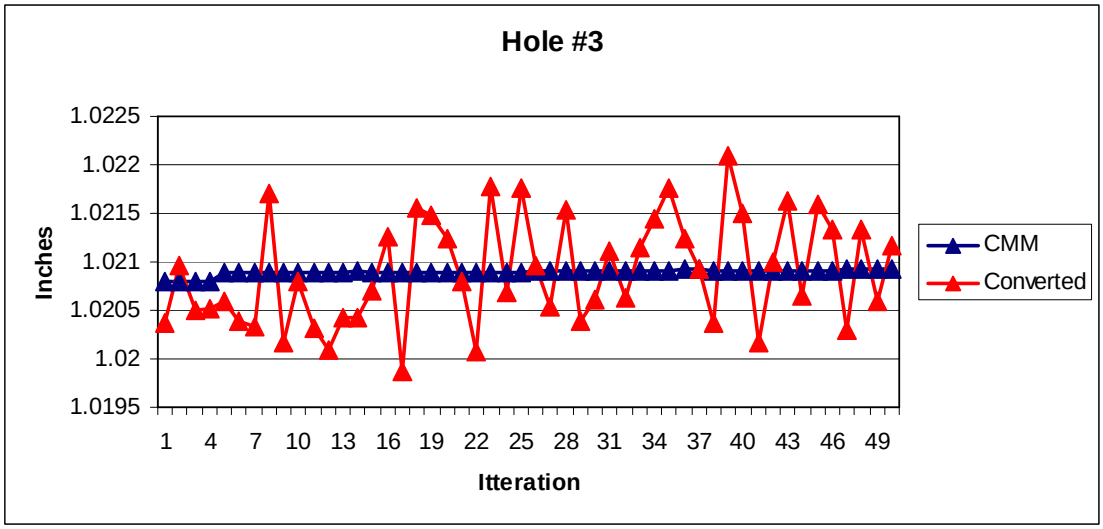

Figure 12 – Hole #3 Data

Mean	Mean	Convert			
0.520205	96.122	0.005412			
		Hole #4			
CMM	Raw	Converted	CMM	Raw	Converted
0.520155	96.118	0.520222	0.520226	96.271	0.52105
0.520156	95.97	0.519421	0.52023	96.193	0.520628
0.520087	95.757	0.518268	0.520229	96.343	0.52144
0.520098	96.367	0.52157	0.520231	96.139	0.520336
0.520219	96.483	0.522198	0.520226	95.812	0.518566
0.520226	96.183	0.520574	0.520227	95.835	0.51869
0.520216	96.181	0.520563	0.520228	96.005	0.51961
0.520218	96.238	0.520872	0.520228	95.814	0.518577
0.520218	95.782	0.518404	0.520229	96.337	0.521407
0.520218	95.893	0.519004	0.520227	96.322	0.521326
0.520219	96.108	0.520168	0.52023	96.27	0.521045
0.520222	95.92	0.51915	0.520231	96.127	0.520271
0.520222	95.883	0.51895	0.520231	96.291	0.521158
0.52022	95.799	0.518496	0.520231	96.309	0.521256
0.520221	96.32	0.521315	0.520228	96.13	0.520287
0.520223	96.192	0.520623	0.520226	95.873	0.518896
0.52022	96.44	0.521965	0.520233	96.139	0.520336
0.520222	96.012	0.519648	0.520232	96.353	0.521494
0.52022	96.248	0.520926	0.520231	95.961	0.519372
0.520218	96.335	0.521397	0.520228	96.312	0.521272
0.520222	96.284	0.521121	0.520226	96.255	0.520964
0.52022	96.165	0.520476	0.520228	95.733	0.518138
0.520223	95.854	0.518793	0.520232	95.817	0.518593
0.520218	96.13	0.520287	0.520228	96.212	0.520731
0.520221	96.388	0.521683	0.520223	95.948	0.519302

Table 7 – Hole #4 Data

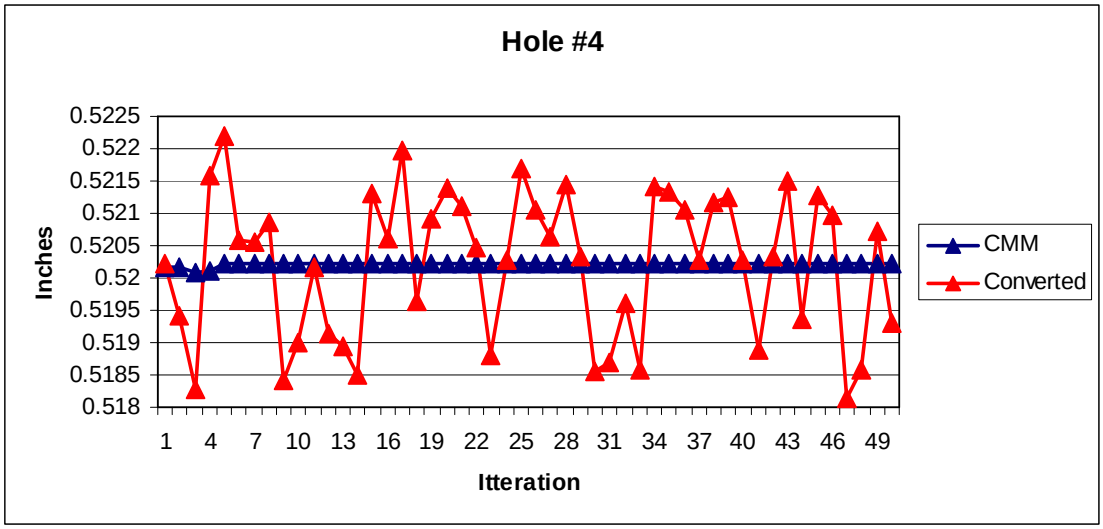

Figure 13 – Hole #4 Data

	Mean	Mean	Convert				
	0.994937	196.4732	0.005064				
			Width #1				
CMM	CMM*	Raw	Converted	CMM	CMM*	Raw	Converted
2.006138	0.995017	196.301	0.993734	2.006107	0.994938	196.651	0.995506
2.006086	0.994943	196.422	0.994347	2.006118	0.994948	196.449	0.994483
2.006088	0.994943	196.534	0.994914	2.006133	0.994956	196.425	0.994362
2.006078	0.994945	196.588	0.995187	2.006117	0.994942	196.496	0.994721
2.006059	0.994938	196.538	0.994934	2.006141	0.994964	196.644	0.99547
2.006086	0.994956	196.226	0.993354	2.006163	0.994986	196.725	0.995881
2.006098	0.994944	196.29	0.993678	2.006129	0.994951	196.477	0.994625
2.006105	0.994948	196.538	0.994934	2.006135	0.994959	196.469	0.994585
2.00607	0.994916	196.502	0.994752	2.006151	0.994971	196.691	0.995708
2.00608	0.994927	196.584	0.995167	2.006146	0.994967	196.578	0.995136
2.006097	0.994941	196.264	0.993547	2.006159	0.994981	196.663	0.995567
2.006088	0.99493	196.351	0.993987	2.006156	0.994978	196.573	0.995111
2.006086	0.994928	196.548	0.994984	2.00614	0.99496	196.485	0.994666
2.006106	0.994941	196.422	0.994347	2.006118	0.994942	196.798	0.99625
2.006102	0.994943	196.503	0.994757	2.006111	0.994936	196.577	0.995131
2.006109	0.994948	196.377	0.994119	2.00611	0.994934	196.722	0.995865
2.006067	0.994917	196.39	0.994185	2.006119	0.994942	196.78	0.996159
2.006072	0.99492	196.554	0.995015	2.00612	0.994943	196.54	0.994944
2.006065	0.99491	196.375	0.994109	2.00615	0.99497	196.563	0.99506
2.00608	0.994927	196.547	0.994979	2.006121	0.994941	196.79	0.99621
2.00609	0.994932	196.544	0.994964	2.006127	0.994946	196.528	0.994883
2.006109	0.994952	196.436	0.994418	2.006144	0.994962	196.49	0.994691
2.006064	0.994911	196.637	0.995435	2.006135	0.994953	196.8	0.99626
2.006089	0.994933	196.613	0.995314	2.00615	0.994966	196.67	0.995602
2.00608	0.994926	196.746	0.995987	2.006157	0.994971	196.614	0.995319

Table 8 – Width #1 Data

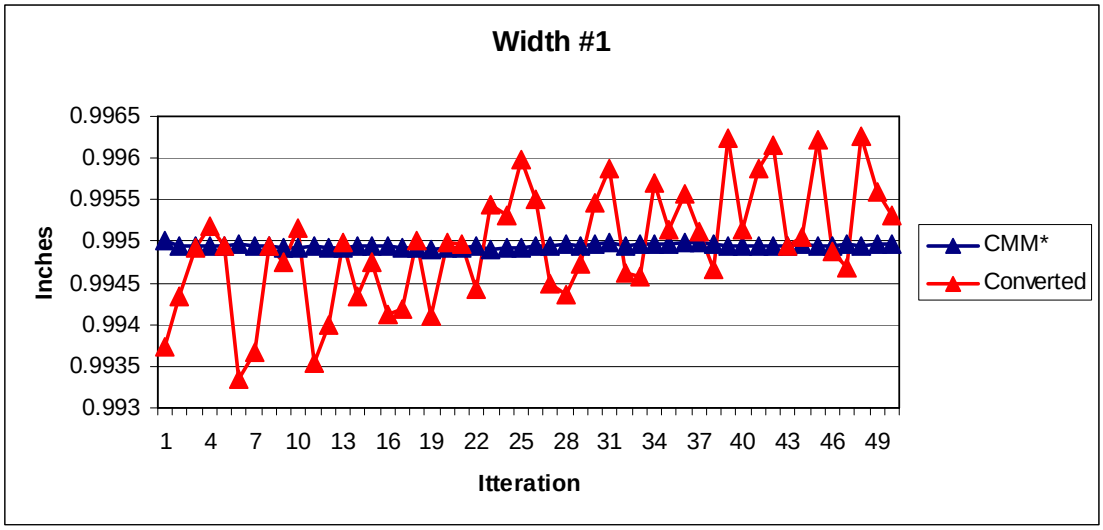

Figure 14 – Width #1 Data

	Mean	Mean	Convert				
	1.244276	248.0863	0.005015				
			Width #2				
CMM	CMM*	Raw	Converted	CMM	CMM*	Raw	Converted
2.005295	1.244345	248.066	1.243932	2.00528	1.244294	248.111	1.244158
2.005231	1.244268	247.907	1.243135	2.005295	1.244307	247.964	1.243421
2.005283	1.244322	248.201	1.244609	2.0053	1.244309	248.177	1.244489
2.005267	1.244309	248.116	1.244183	2.005284	1.244294	248.333	1.245271
2.005244	1.244268	248.098	1.244093	2.005296	1.244307	248.139	1.244298
2.00523	1.244254	247.924	1.24322	2.005309	1.244319	248.316	1.245186
2.005248	1.244274	247.953	1.243366	2.005294	1.244303	248.208	1.244644
2.005255	1.244279	248.213	1.244669	2.005295	1.244304	248.112	1.244163
2.005237	1.244259	248.036	1.243782	2.005298	1.244308	248.269	1.24495
2.005245	1.244267	248.148	1.244343	2.005296	1.244306	248.009	1.243646
2.005247	1.244267	248.094	1.244073	2.005301	1.244309	248.292	1.245066
2.005251	1.244273	248.262	1.244915	2.005294	1.244301	247.992	1.243561
2.005255	1.244278	248.158	1.244394	2.005291	1.2443	248.044	1.243822
2.005247	1.244265	248.02	1.243702	2.005287	1.244299	248.105	1.244128
2.00526	1.244282	248.179	1.244499	2.005281	1.244291	248.191	1.244559
2.005255	1.244278	248.111	1.244158	2.00528	1.24429	248.035	1.243777
2.005233	1.24426	247.98	1.243501	2.005289	1.244298	248.349	1.245351
2.005237	1.244263	248.046	1.243832	2.005281	1.24429	248.118	1.244193
2.005229	1.244255	247.984	1.243521	2.005306	1.244313	248.386	1.245537
2.005249	1.244274	248.043	1.243817	2.005291	1.244298	248.356	1.245387
2.005251	1.244276	247.966	1.243431	2.005291	1.244298	248.329	1.245251
2.005258	1.244282	248.16	1.244404	2.005303	1.24431	248.357	1.245392
2.005234	1.244258	248.177	1.244489	2.005301	1.244306	248.207	1.244639
2.005247	1.244274	248.244	1.244825	2.005309	1.244314	248.146	1.244333
2.005245	1.244271	248.071	1.243957	2.005312	1.244318	248.163	1.244419

Table 9 – Width #2 Data

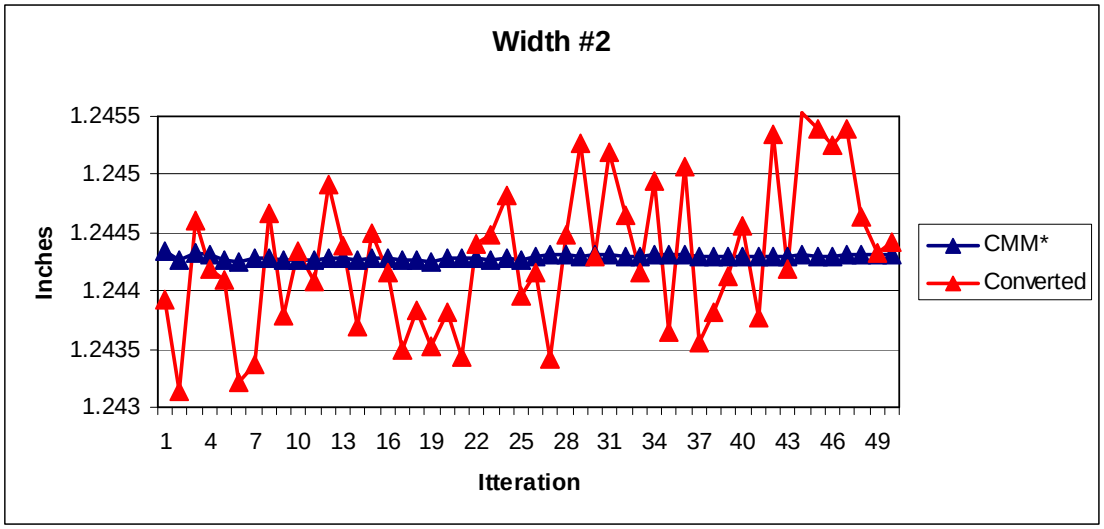

Figure 15 – Width #2 Data

	Mean	Mean	Convert				
	1.493769	298.2524	0.005008				
			Width #3				
CMM	CMM*	Raw	Converted	CMM	CMM*	Raw	Converted
2.004322	1.493922	298.314	1.493779	2.004237	1.493783	298.268	1.493548
2.004326	1.493928	298.304	1.493729	2.004251	1.493797	298.17	1.493058
2.004239	1.493837	298.096	1.492687	2.00426	1.493802	298.307	1.493744
2.004231	1.493828	298.183	1.493123	2.00424	1.493784	298.266	1.493538
2.004196	1.493753	298.053	1.492472	2.004238	1.493782	298.343	1.493924
2.004167	1.493721	298.299	1.493703	2.004246	1.49379	298.499	1.494705
2.004182	1.493737	298.349	1.493954	2.004239	1.493782	298.139	1.492902
2.004185	1.493739	298.404	1.494229	2.00424	1.493783	298.522	1.49482
2.004189	1.493742	298.114	1.492777	2.004237	1.493779	298.169	1.493053
2.004197	1.493751	298.107	1.492742	2.004233	1.493775	298.472	1.49457
2.004198	1.49375	298.247	1.493443	2.004238	1.49378	298.175	1.493083
2.004208	1.493762	298.281	1.493613	2.004232	1.493774	298.411	1.494264
2.004208	1.49376	298.158	1.492997	2.004234	1.493776	298.509	1.494755
2.004184	1.493734	298.324	1.493829	2.004237	1.49378	298.574	1.495081
2.004205	1.493757	298.327	1.493844	2.004233	1.493776	298.239	1.493403
2.004194	1.493746	298.401	1.494214	2.004233	1.493776	298.485	1.494635
2.004191	1.493746	298.112	1.492767	2.004243	1.493786	298.534	1.49488
2.004196	1.49375	298.402	1.494219	2.004237	1.49378	298.521	1.494815
2.004191	1.493744	298.166	1.493037	2.004241	1.493785	298.558	1.495
2.004205	1.493759	298.171	1.493063	2.004241	1.493784	298.308	1.493749
2.004193	1.493746	298.374	1.494079	2.00425	1.493792	298.334	1.493879
2.004198	1.493751	298.12	1.492807	2.004254	1.493795	298.344	1.493929
2.004195	1.493748	298.418	1.494299	2.004253	1.493793	298.424	1.494329
2.004195	1.493749	298.183	1.493123	2.004255	1.493796	298.337	1.493894
2.004203	1.493757	298.403	1.494224	2.004257	1.493798	298.465	1.494535

Table 10 – Width #3 Data

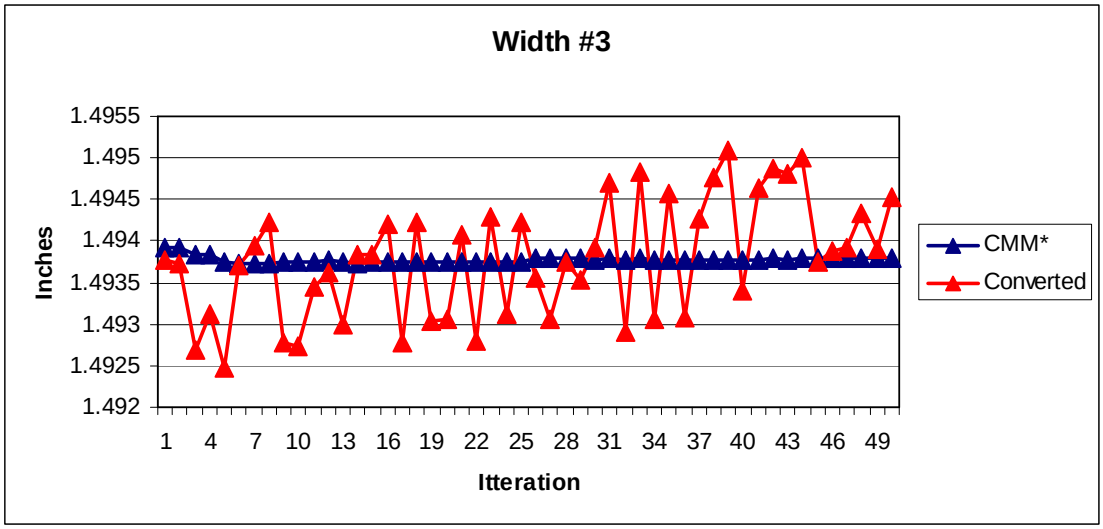

Figure 16 – Width #3 Data

	Mean	Mean	Convert				
	1.743147	347.4408	0.005017				
			Width #4				
CMM	CMM*	Raw	Converted	CMM	CMM*	Raw	Converted
2.003269	1.743191	347.41	1.742331	2.003278	1.743165	347.688	1.743725
2.003284	1.743206	347.059	1.74057	2.003289	1.743174	347.519	1.742877
2.003373	1.743329	347.487	1.742717	2.003313	1.743198	347.747	1.744021
2.003372	1.743323	347.451	1.742536	2.0033	1.743185	347.63	1.743434
2.00324	1.74313	347.147	1.741012	2.003276	1.743163	347.715	1.74386
2.00321	1.743097	347.228	1.741418	2.003284	1.743171	347.701	1.74379
2.003212	1.743104	347.284	1.741699	2.003278	1.743164	347.477	1.742667
2.003218	1.743109	347.426	1.742411	2.003277	1.743163	347.649	1.743529
2.003234	1.743126	347.551	1.743038	2.003273	1.743159	347.719	1.74388
2.003246	1.743137	347.39	1.74223	2.00327	1.743156	347.707	1.74382
2.00325	1.743141	347.626	1.743414	2.003278	1.743163	347.737	1.743971
2.003253	1.743142	347.212	1.741338	2.003275	1.74316	347.836	1.744467
2.003254	1.743143	347.346	1.74201	2.003275	1.743159	347.76	1.744086
2.003234	1.743124	347.222	1.741388	2.003282	1.743167	347.805	1.744312
2.00324	1.74313	347.63	1.743434	2.003286	1.743172	347.811	1.744342
2.003221	1.74311	347.633	1.743449	2.003286	1.743173	347.668	1.743624
2.003241	1.743132	347.335	1.741954	2.003284	1.743167	347.843	1.744502
2.003237	1.743126	347.57	1.743133	2.003283	1.743167	347.822	1.744397
2.003242	1.743132	347.454	1.742551	2.003283	1.743168	347.627	1.743419
2.003244	1.743135	347.562	1.743093	2.003289	1.743174	347.849	1.744532
2.003225	1.743114	347.476	1.742662	2.003298	1.743185	347.559	1.743078
2.003228	1.743118	347.475	1.742657	2.003302	1.743188	347.826	1.744417
2.003235	1.743124	347.651	1.743539	2.003309	1.743194	347.891	1.744743
2.003236	1.743127	347.672	1.743645	2.003307	1.743193	347.606	1.743314
2.003242	1.743131	347.723	1.7439	2.003301	1.743189	347.556	1.743063

Table 11 – Width #4 Data

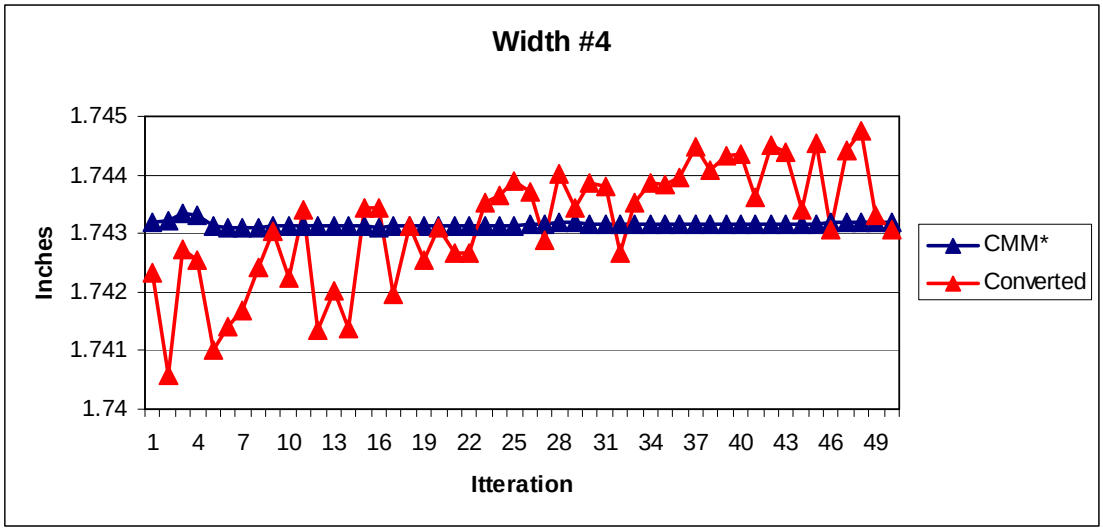

Figure 17 – Width #4 Data

CHAPTER FIVE: ANALYSIS & CONCLUSION

In order to properly analyze the data the appropriate tests and corresponding hypotheses must be established. The first step was to determine the type of data being analyzed. The data from this experiment is continuous and not assumed to be normally distributed. Having data that is not normally distributed requires the use of nonparametric methods to evaluate the variance. Levene's test was used for this experiment. Unlike the F-Test, Levene's test evaluates each of the iterations against the sample median instead of the sample mean. The null and alternative hypotheses, for all sets of data, are as follows:

$$H_o : \sigma_1 = \sigma_2 \qquad H_a : \sigma_1 \neq \sigma_2$$

The gathered data was entered into Minitab and used to generate Individual Value Plots and to run tests for equal variance (Levene's test). These can be found on the pages that follow. The value plots show another view of the same data graphed in Chapter 4. The graphical representations of the tests for equal variance include the results of the Levene's tests, Bonferroni confidence intervals, and box plots of the data sets.

The Bonferroni method is used to control the overall confidence level when dealing with multiple confidence intervals. Bonferroni confidence intervals are slightly wider than normal confidence intervals, but limit the maximum total error rate to α. The normal confidence intervals use the confidence coefficient (1 – α), while the Bonferroni intervals use (1 – α / g), where 'g' equals the total number of intervals. For this experiment, each interval has a confidence interval of 97.5% (1 – 0.05 / 2) achieving an overall confidence level of at least 95%.

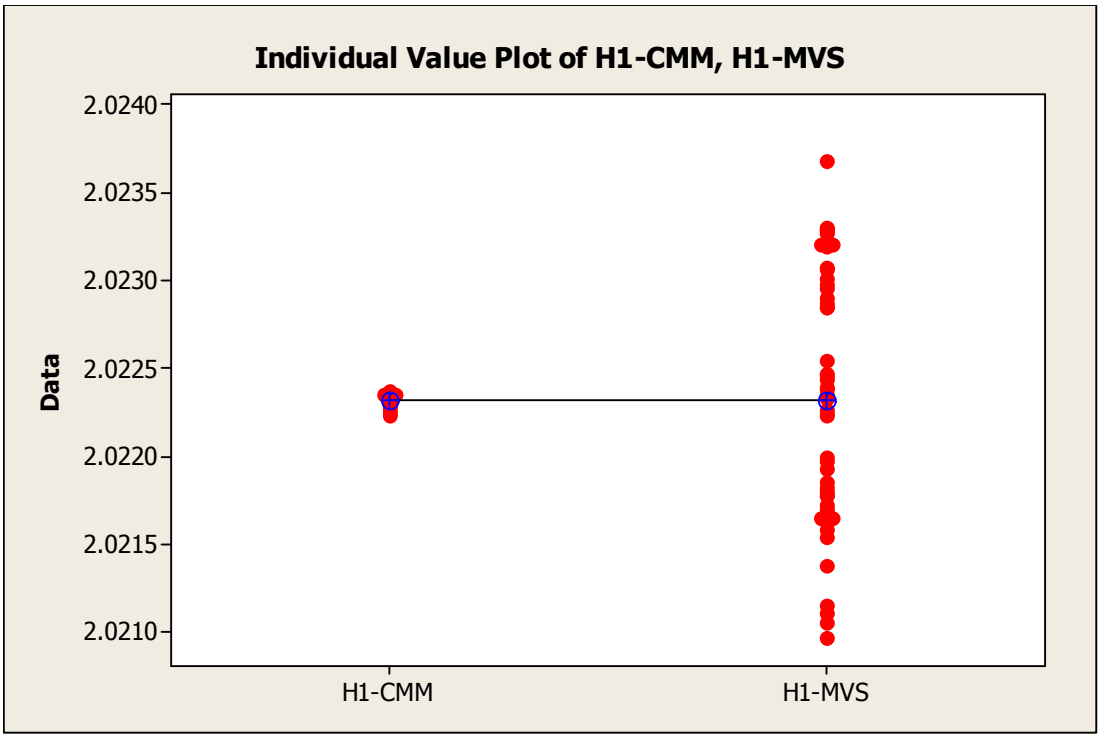

Figure 18 – Individual Value Plot for Hole #1

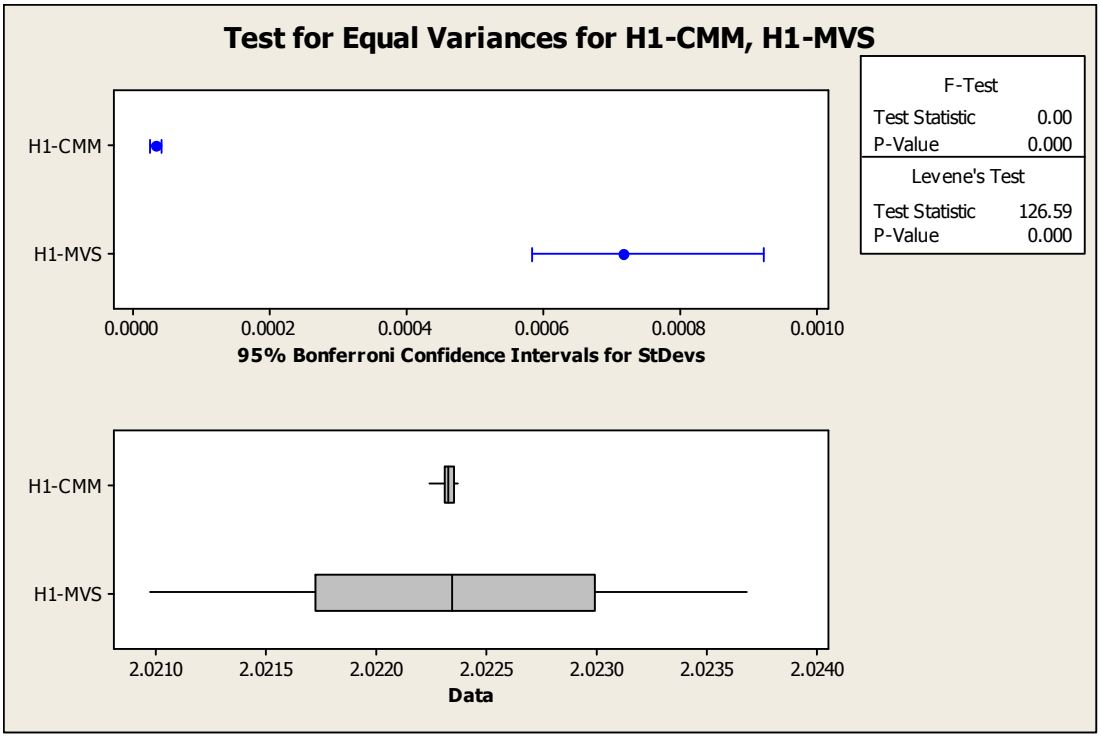

Figure 19 – Test for Equal Variances for Hole #1

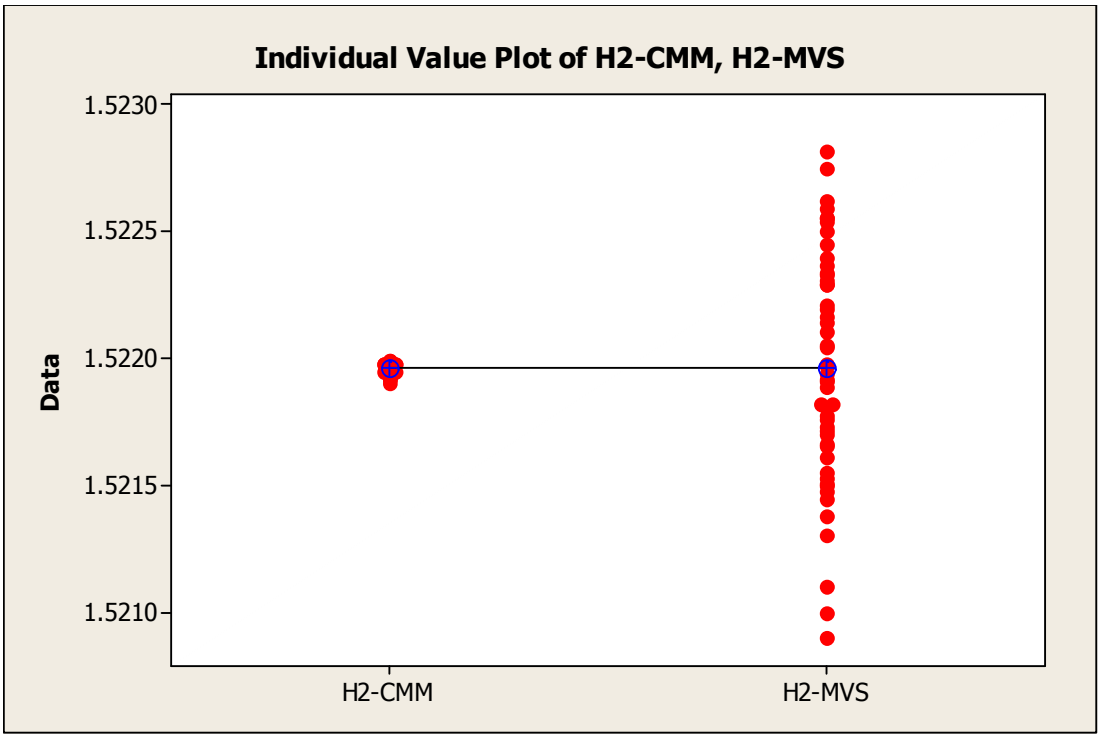

Figure 20 – Individual Value Plot for Hole #2

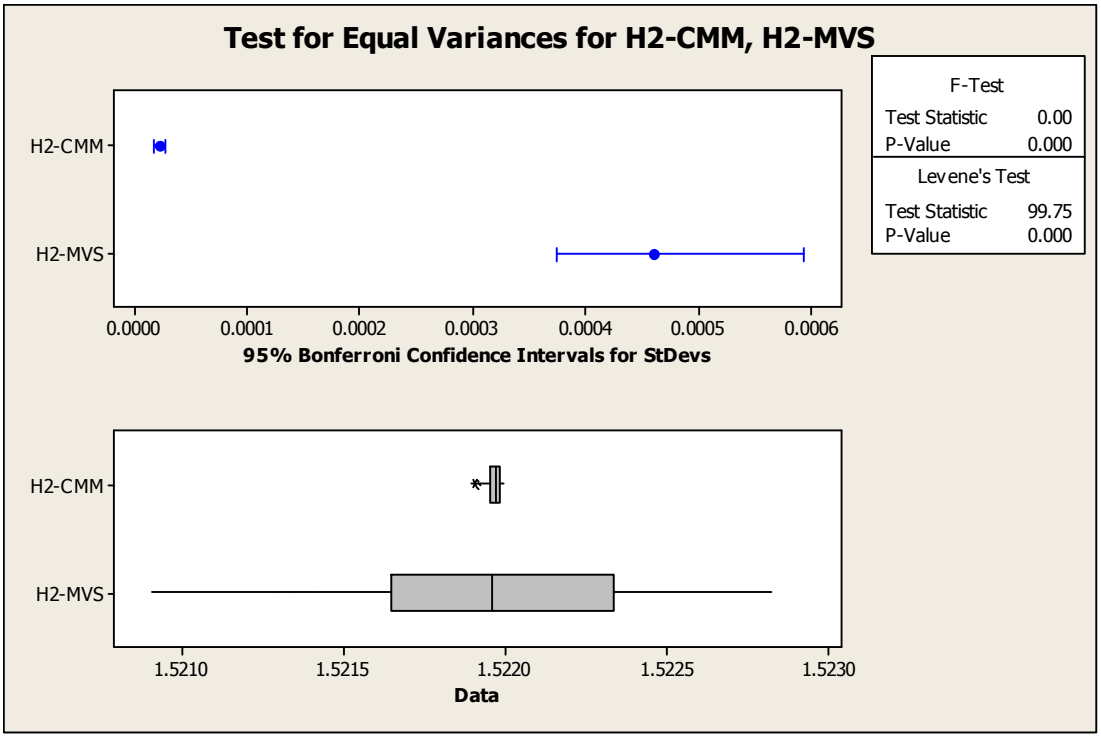

Figure 21 – Test for Equal Variances for Hole #2

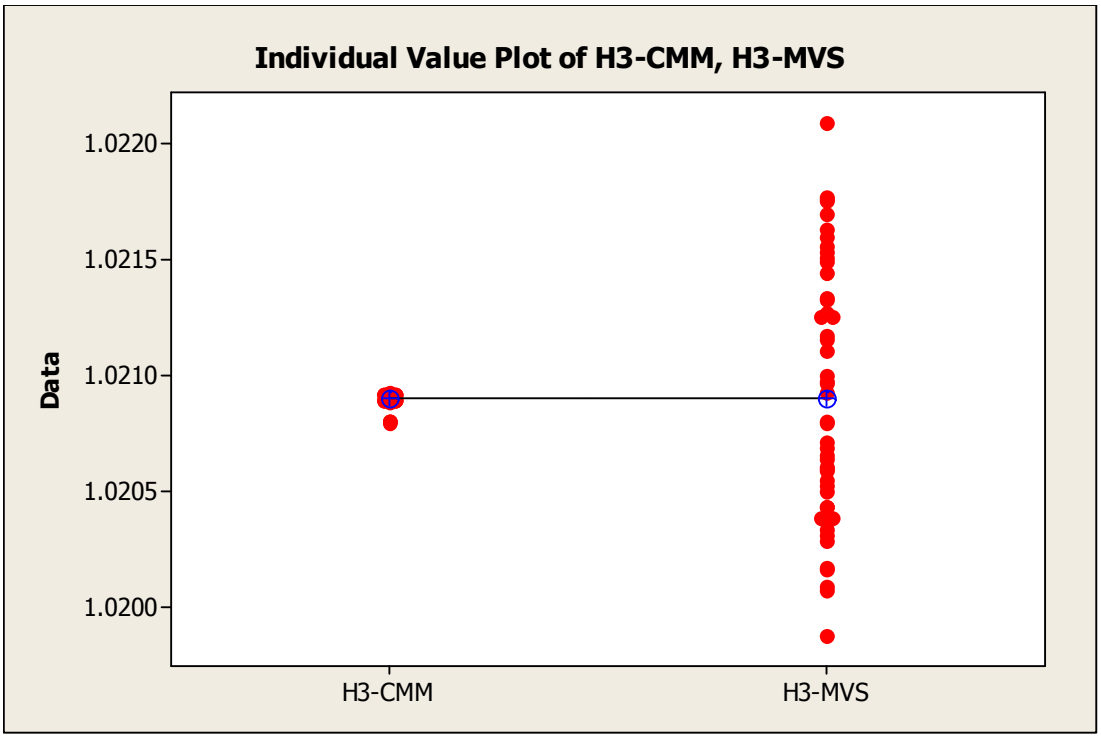

Figure 22 – Individual Value Plot for Hole #3

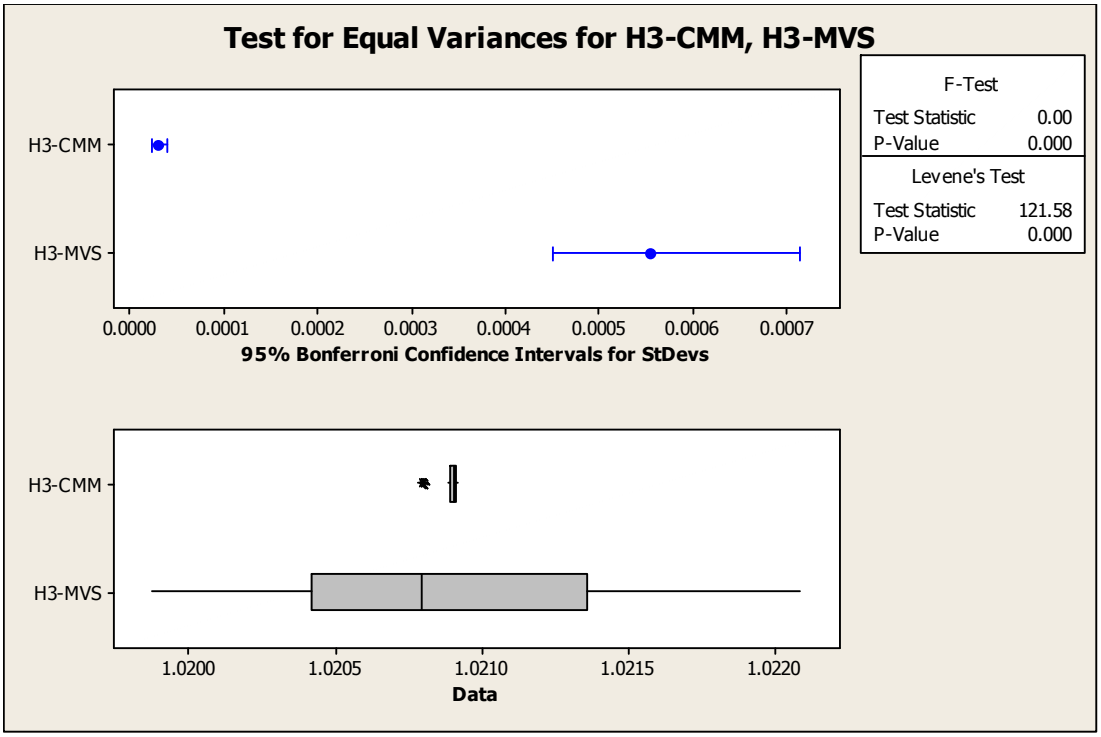

Figure 23 – Test for Equal Variances for Hole #3

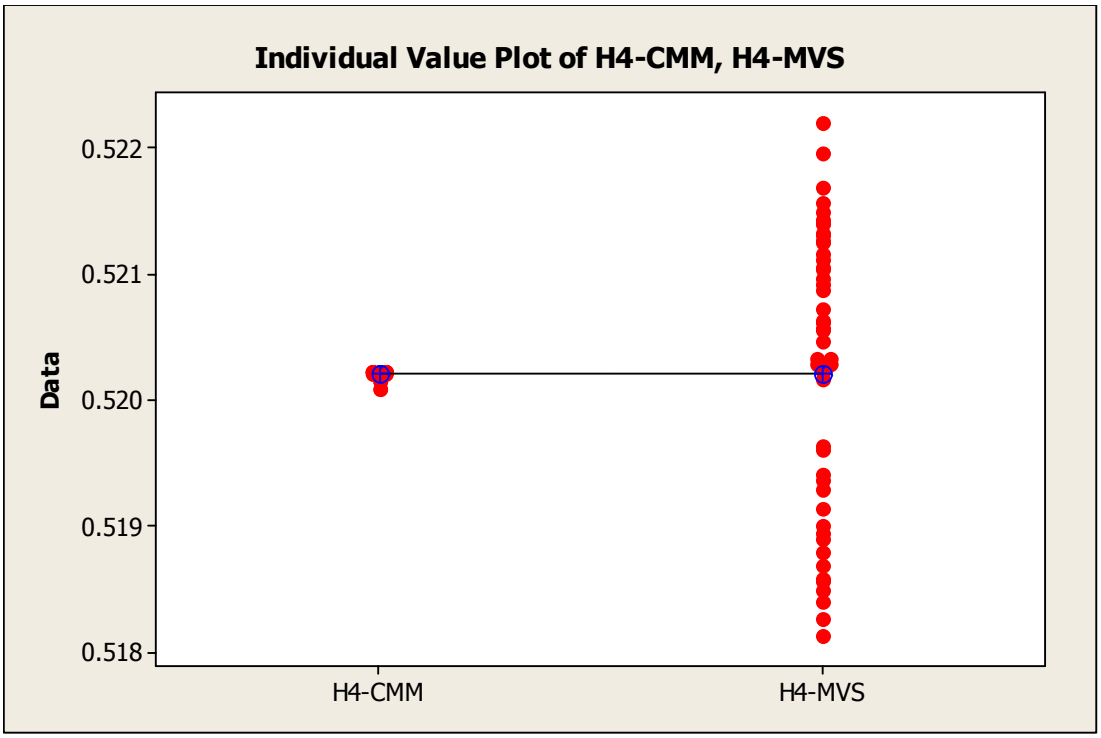

Figure 24 – Individual Value Plot for Hole #4

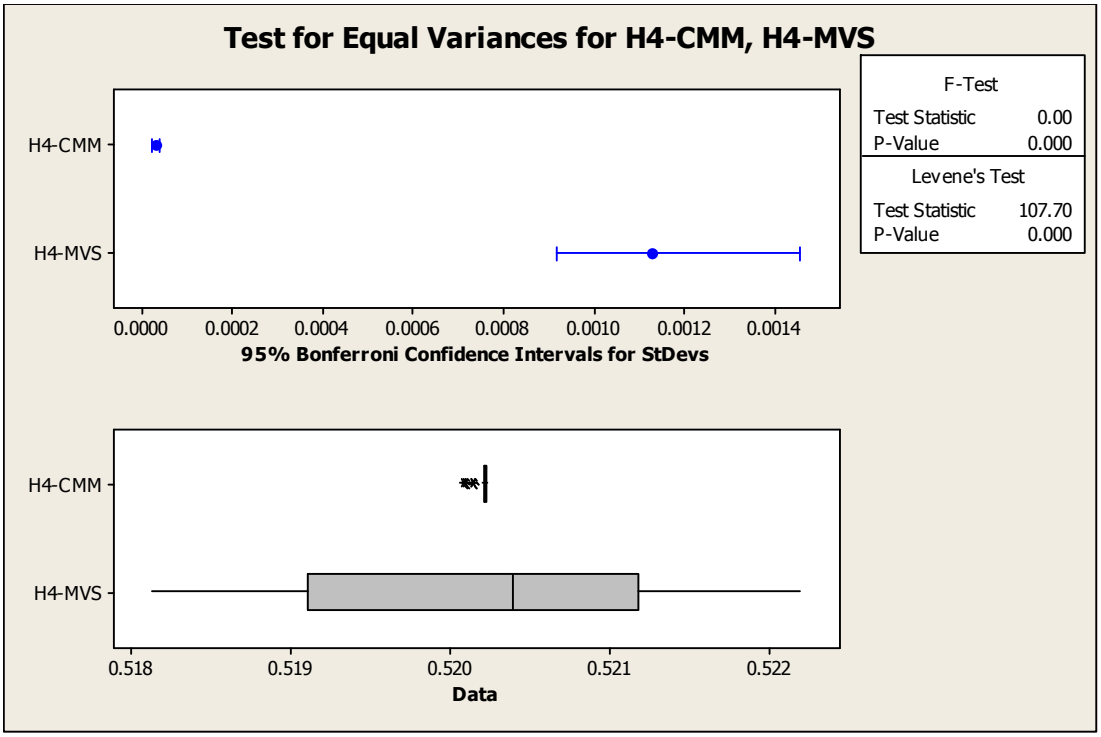

Figure 25 – Test for Equal Variances for Hole #4

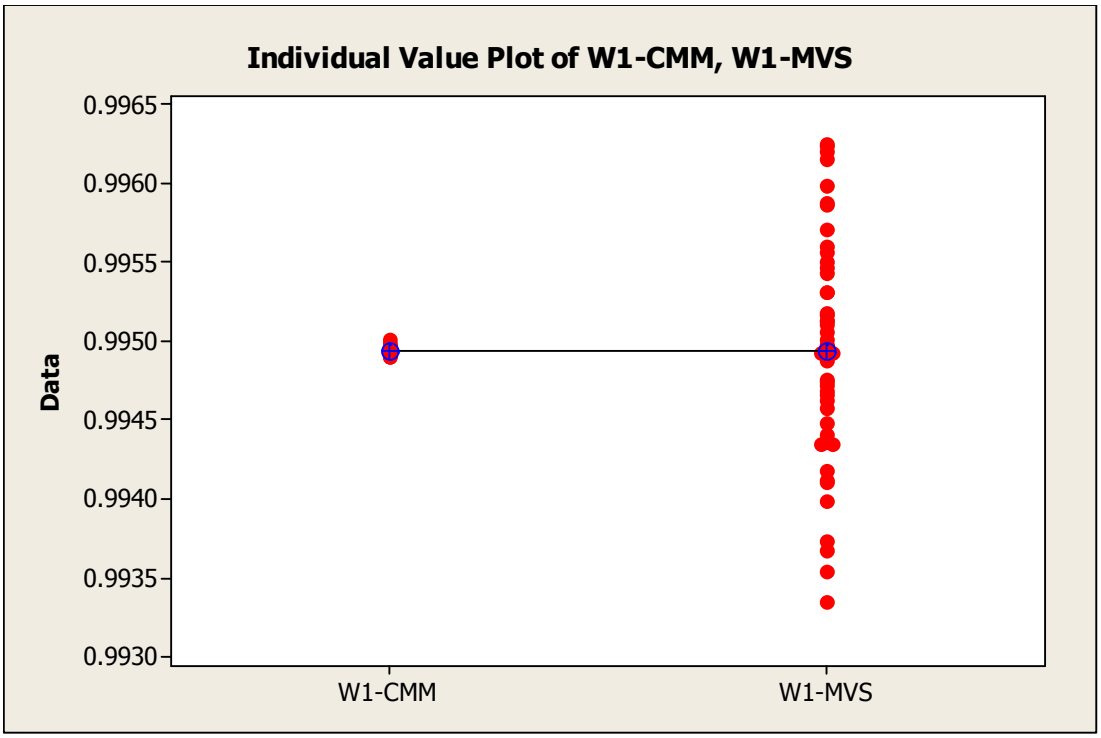

Figure 26 – Individual Value Plot for Width #1

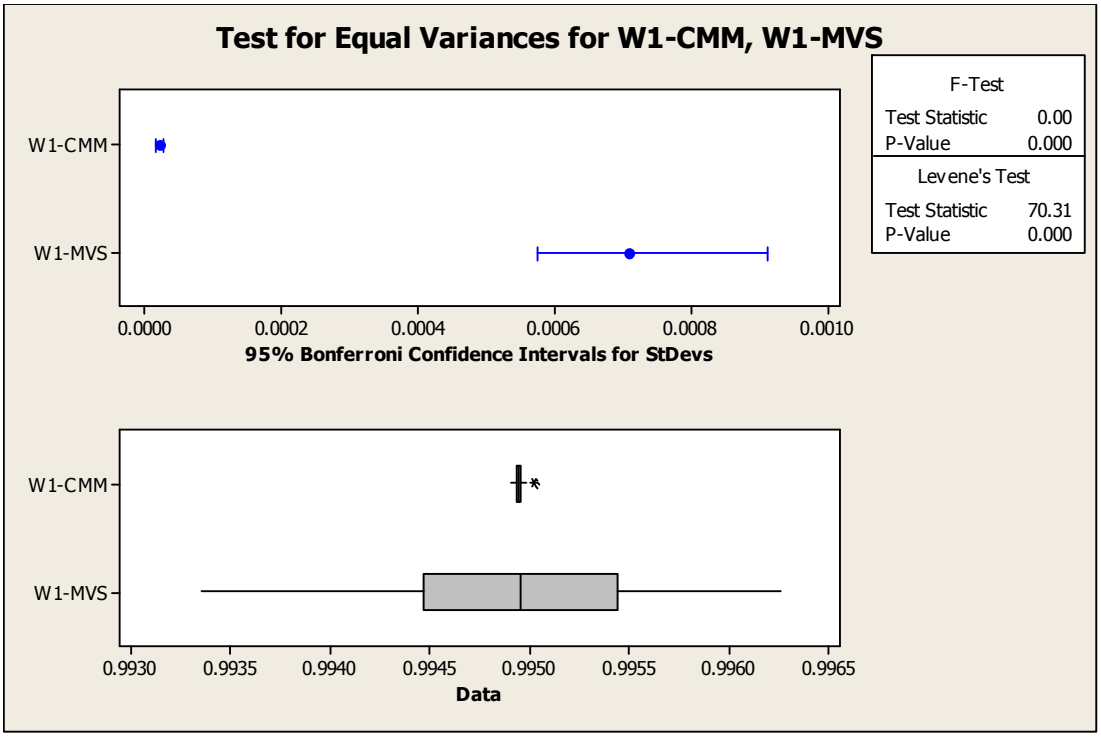

Figure 27 – Test for Equal Variances for Width #1

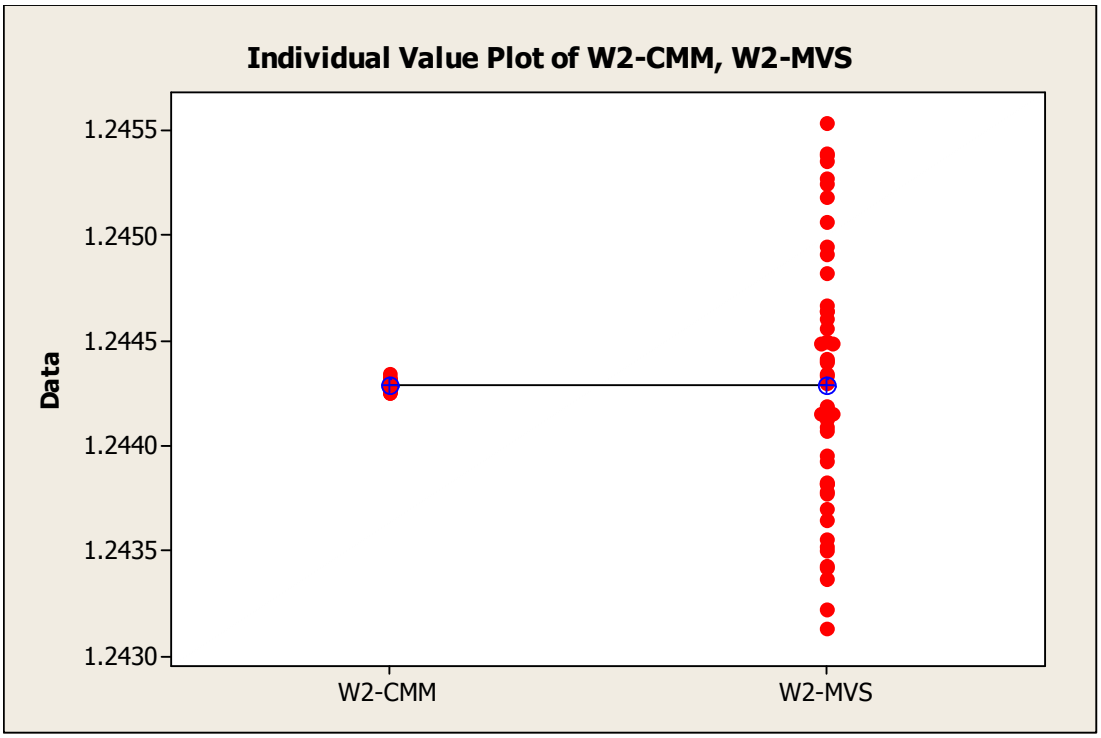

Figure 28 – Individual Value Plot for Width #2

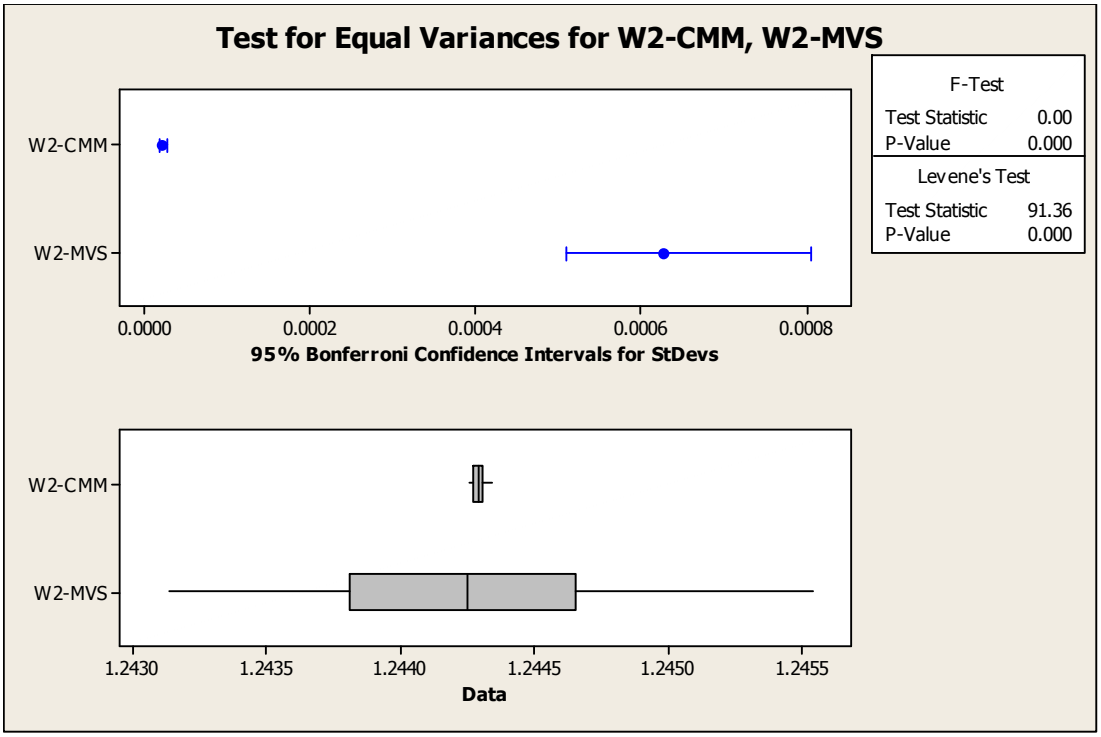

Figure 29 – Test for Equal Variances for Width #2

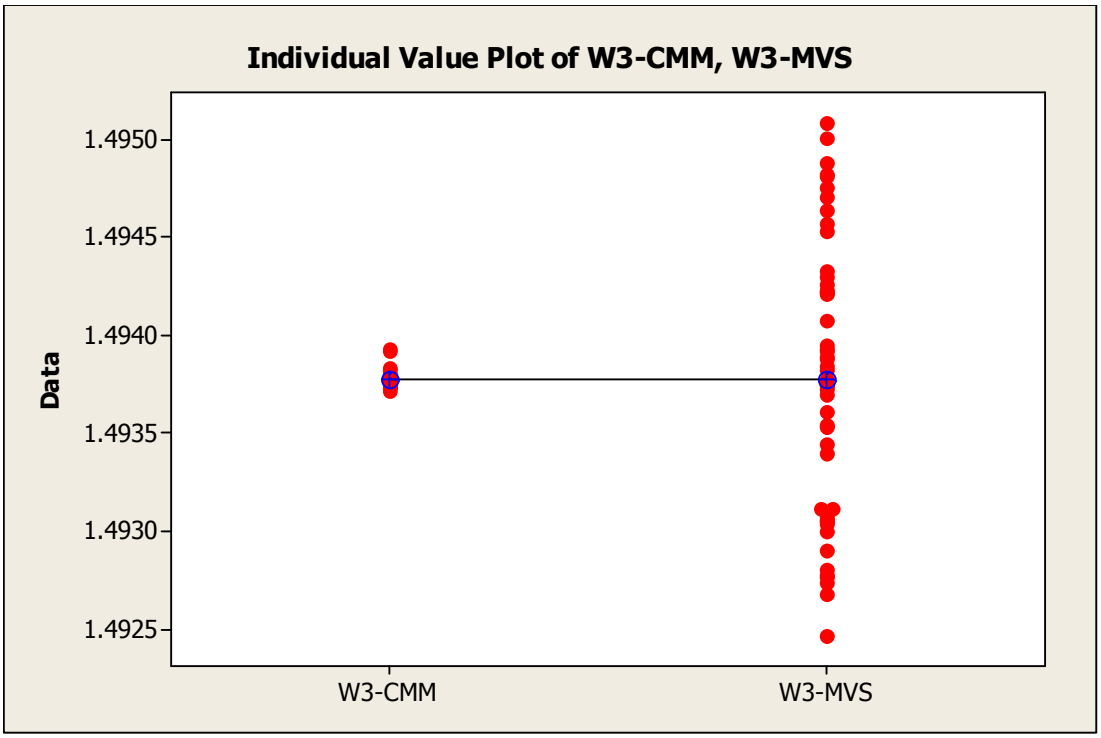

Figure 30 – Individual Value Plot for Width #3

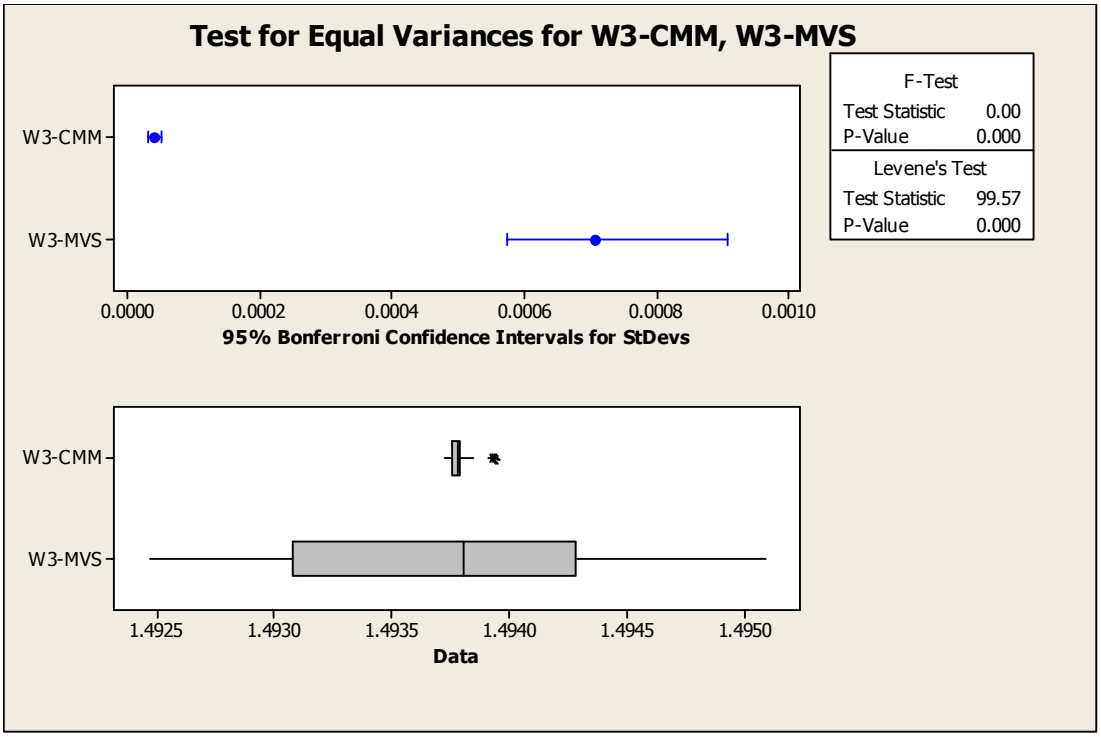

Figure 31 – Test for Equal Variances for Width #3

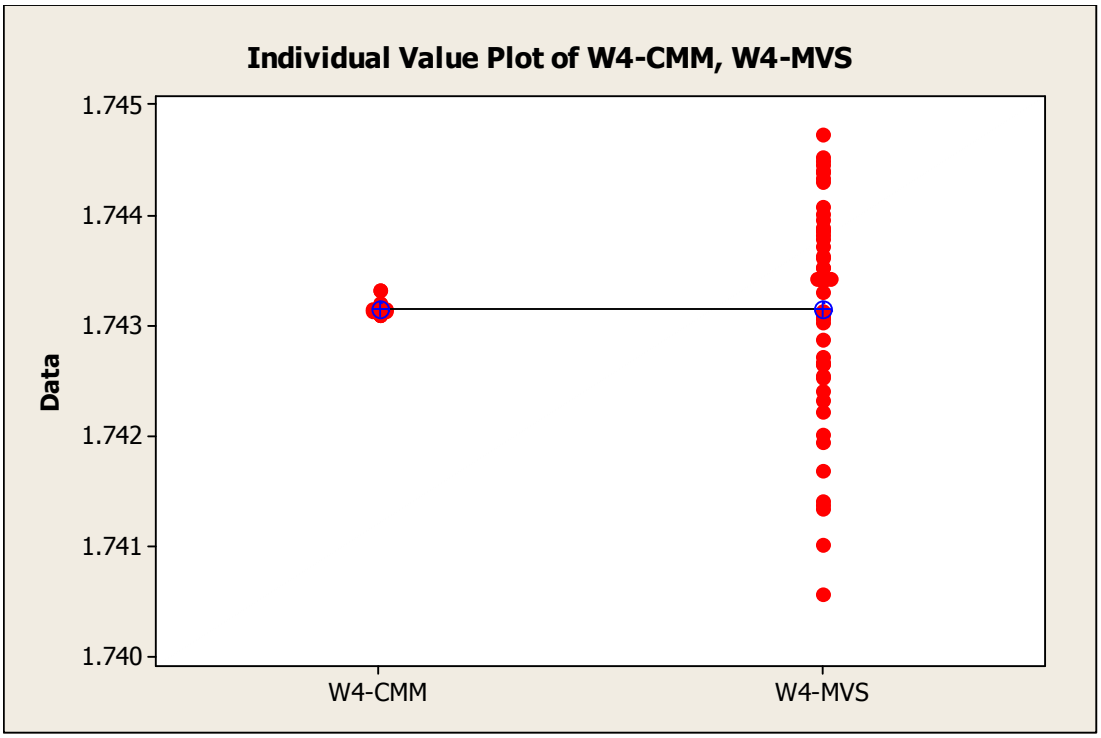

Figure 32 – Individual Value Plot for Width #4

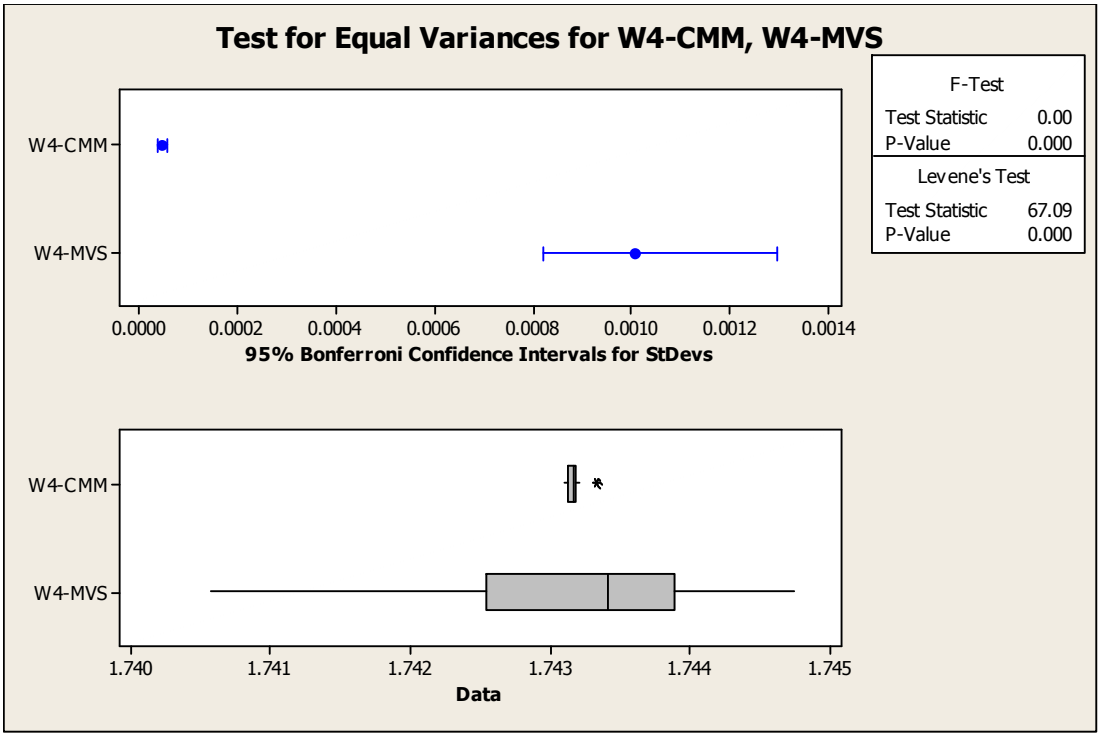

Figure 33 – Test for Equal Variances for Width #4

The Levene's tests for all sets of data show that the P-Value is less than 0.0001, which is less than the α-value (0.05). As a result, the null hypothesis is rejected and the alternative hypothesis is accepted. This result means that the accuracy and repeatability of the Keyence MVS is not equal to that of the Zeiss CMM. Using the graphical data, it is easy to see that the measurements taken with the CMM vary much less than those taken with the MVS, making the CMM the better choice for gathering measurement data. This conclusion remained true when the degree of accuracy was reduced, from 7 decimal places down to 4. The results of this test are displayed in the figure below. Reducing the degree of accuracy further would invalidate the data. It can be concluded that the measurements gathered by the MVS are not comparable to those of the CMM at any level of accuracy. Improvements to the MVS setup must be made to improve accuracy.

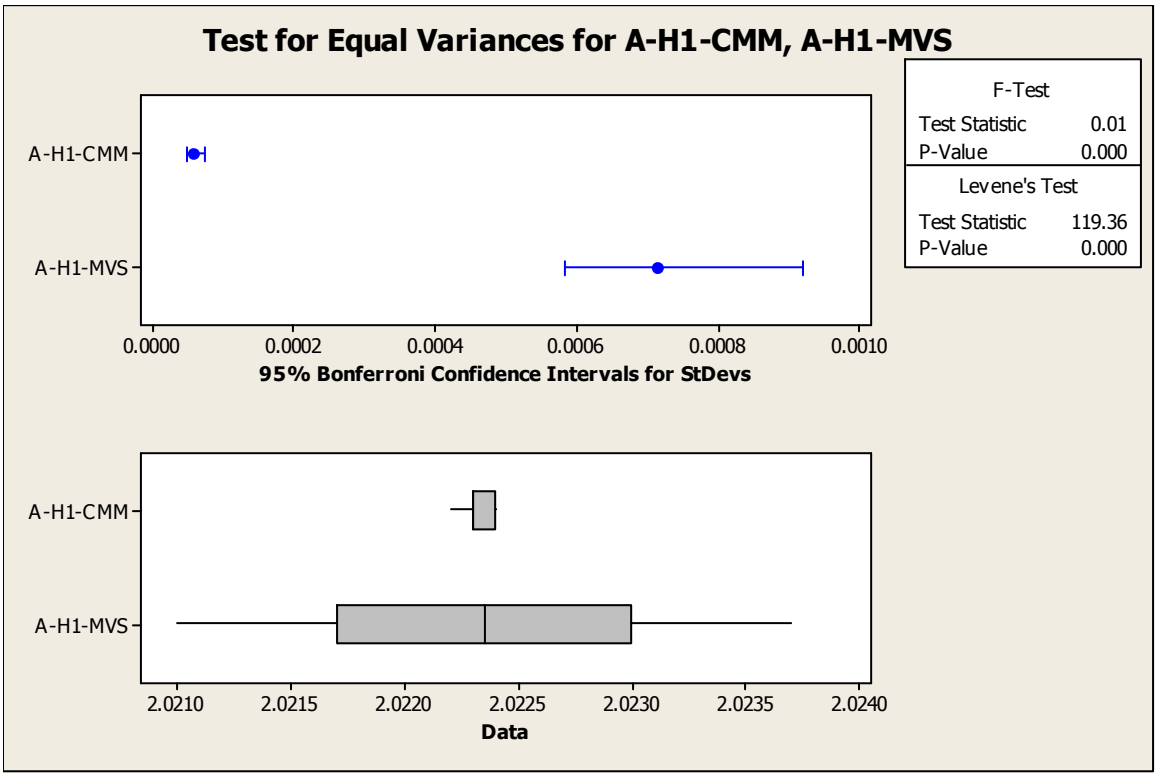

Figure 34 – Test for Equal Variances for Hole #1 (Reduced Accuracy)

FUTURE WORK

The data gathering process drew attention to variables that need to be addressed in order to improve the accuracy of the vision system. The original jig was constructed to be adjustable and portable. This was necessary to establish a good focal distance, and for relocating the project when needed. A fixed jig should be implemented for future work, to eliminate any movement of the camera.

The lighting was selected with the same concept in mind, adjustable and portable. As mentioned before, clamp lighting was used to illuminate the target object. These lights were inexpensive, easy to implement, provided adequate lighting, and were easily adjusted. During preliminary experiments, it was discovered that moving or adjusting the lights the slightest amount would skew the pixel output of the MVS. For any future work it is absolutely necessary that the lighting, once properly positioned, is locked in place to prevent any movement.

The nature of the power used for the lighting was also an issue. As discussed before, a preliminary experiment was conducted to reduce any sinusoidal fluctuation, or “ripple”, present in the lighting. Although greatly reduced, the existence of ripple was still observed. In order to eliminate this ripple, the power source must be changed to a constant DC source. This can be done by employing a rectifier or a battery pack and using a voltage regulator for added protection.

The preliminary experiment tested three different bulb types (light sources). The bulb that was ultimately chosen (halogen) produced the least amount of ripple of the three, but was not necessarily the best light source that can be used. Research suggests that LED light sources produce little to no ripple. This is due to the fact that the LED current is exponential to the voltage, meaning that a small change in voltage creates a large change in the current. A power converter (or switched-mode power supply) should be used to ensure that the LED will work properly and not be damaged. For this particular camera setup the use of LED ring lighting is suggested for the best results. An apparatus designed specifically for this MVS can be purchased from the manufacturer (Keyence).

The last issue that arose was the test part itself. The material that the test part was milled from turned out to be a poor choice. The ABS material was used because it was readily available and a new test part could be milled at anytime, without the need to order more material. The original test part was milled out of aluminum. When another test part was needed, with different features, the aluminum stock used to mill the first part was gone. The heat sensitivity of the aluminum was not an issue when running the preliminary tests and the problems that arose from using ABS were not expected. Any new test parts should be sturdy, resistant to heat, and produce little glare. The features chosen for the test part proved to be adequate; however, for future experiments, more shapes should be tested.

REFERENCES

AcaStat Software (2009). Research methods handbook. AcaStat Software Web site: http://www.acastat.com/Handbook/Contents.html

Adept Electronic Solutions (2005). Industry news archive - 2005. Adept Electronic Solutions Web site: http://www.adept.net.au/news/2005_news/2005-archive.shtml

Batchelor, B. G., & Charlier, J. (1998). Machine vision is not computer vision. *SPIE Conf. on MVS for Inspection and Metrology VII*, *3521*, 2-13.

Bennedsen, B. S., Peterson, D. L., & Tabb, A. (2005). Identifying defects in images of rotating apples. *Computers and Electronics in Agriculture. 48*, 92-102.

Bhatia, G., Godhwani, A., & Grindon, J. (1991). Optimal 3D surface metrology-localization of fiducial points. *IEEE Proceedings of Southeastcon '91*. *2*, 925-930.

Carl Zeiss, Inc. (2008). Industrial Metrology. Carl Zeiss IMT Web site: http://www.zeiss.com/IMT

Chen, Y., Chao, K., & Kim, M. S. (2002). Machine vision technology for agricultural *applications. Computers and Electronics in Agriculture. 36*, 173-191.

Conklin, C., Watkins, R., Foo, S., Brooks, G., Roberts, R., & Perry, R. (2002). Dichromatic color perception: a fast alternative for machine vision systems. *Engineering Applications of Artificial Intelligence. 15*, 351-355.

Criminisi, A., Reid, I., & Zisserman, A. (1999). Single view metrology. *The Proceedings of the Seventh IEEE International Conference on Computer Vision, 1999. 1*, 434-441.

Diamond, W. J. (1989). *Practical experimental designs for engineers and scientists*. New York, New York, USA: Van Nostrand Reinhold.

Edmund Optics (2009). Choosing the correct illumination. Technical Support - Edmund Optics Web site: http://www.edmundoptics.com/techSupport/DisplayArticle.cfm?articleid=264

Edmund Optics (2009). Frequently asked questions on illumination. Technical Support - Edmund Optics Web site: http://www.edmundoptics.com/techSupport/DisplayArticle.cfm?articleid=276

Einhäuser, W., Hipp, J., Eggert, J., Körner, E., & König, P. (2005). Learning viewpoint invariant object representation using a temporal coherence principle. *Biological Cybernetics. 93*, 79-90.

Ehrenman, G. (2005).Eyes on the line. *Mechanical Engineering. 127,* 25-27.

Evans, J. R., & Lindsay, W. M. (2005). *The management and control of quality.* Mason, Ohio, USA: Thomson South-Western.

Hamada, M. (2002).The advantages of continuous measurements over pass/fail data. *Quality Engineering. 15,* 253-258.

iSixSigma (2008). What is Six Sigma? iSixSigma Web site: http://www.isixsigma.com/sixsigma/six_sigma.asp

Jurkovic, J., Korosec, M., & Kopac, J. (2005). New approach in tool wear measuring technique using CCD vision system. *International Journal of Machine Tools and Manufacture. 45,* 1023-1030.

Keyence, Co. (2001). Machine Vision Encyclopedia [CD-ROM]. Osaka, JP: Keyence Corporation.

Keyence, Co. (2006). *Super-high-speed digital machine vision supporting multi-camera CV-3002 series user's manual.* Osaka, JP: Keyence Corporation.

Keyence, Co. (2008). Sensors, vision, measurement, and microscopes. Keyence Global Home Web site: http://www.keyence.com/

Köthe, U., & Neumann, B. (2005). Computer Vision: Bildverarbeitung Web site: http://kogs-www.informatik.uni-hamburg.de/~neumann/BV-SS-2005/BV-Woche1-05.pdf

Lavest, J. M., Viala, M., & Dhome, M. (1998). Do we really need an accurate calibration pattern to achieve a reliable camera calibration? *Proc. Eur. Conf. Comput. Vis., Freiburg, Germany, 1998,* 158-174

Ling, R. (1994). On MNCP in two-stage technique for 3D camera calibration for machine vision metrology. *1994 International Symposium on Speech, Image Processing, and Neural Networks.* 77-80.

Mendonça, P. R. S., & Kaucic, R. (2008). Single view metrology: a practical example. *IEEE Workshop on Applications of Computer Vision.* 1-8.

Mercron (2008). Common problems. Machine Vision Light solutions – Mercron Web site: http://www.mercron.com/questions.htm

Minitab Inc. (2006). Minitab Statistical Software, Release 15 for Windows. State College, Pennsylvania, USA: Minitab Inc.

Morse, E. P. (2002). Artifact selection in its role in CMM evaluation. Web site: http://www.coe.uncc.edu/~emorse/research/papers/IDW%202002.pdf

Natrella, M. (2003). *NIST/SEMATECH e-Handbook of Statistical Methods*. U.S. Commerce Department's Technology Administration Web site: http://www.itl.nist.gov/div898/handbook/

Novini, A. (1993). Fundamentals of machine vision lighting. *WESCON/'93. Conference Record.* 44-52

Os, A., Bae, C., & Merritt, J. (2007). Computer Vision Web site: http://library.thinkquest.org/06aug/00593/history.html

Pastorius, W. J. (1988). Machine vision for industrial inspection metrology and guidance. *Fourth Annual Canadian Programmable Control and Automation Technology Conference and Exhibition. 13A-1*, 1-5.

Purdue University Online Writing Lab (OWL) (2008). APA Formatting and Style Guide. Web site: http://owl.english.purdue.edu/owl/resource/560/01/

Rahman, S. (2005). *Obstacle detection for mobile robots using computer vision.* Unpublished master's thesis, University of York, Heslington, York, UK.

Ramadan, A. (2006, July 17). PN Diodes. Hari's Corner Web site: http://haribrahma.wordpress.com/2008/09/

Renaud, P., Andreff, N., Lavest, J. M., & Dhome, M. (2006). Simplifying the kinematic calibration of parallel mechanisms using vision-based metrology. *IEEE Transactions on Robotics. 22*, 12-22.

Repas, R. (2008).Lighting the way for vision. *Machine Design. Feb. 21*

Roberts, L. G. (1965). *Machine perception of three-dimensional solids.* Unpublished master's thesis, Massachusetts Institute of Technology, Cambridge, Massachusetts, USA.

Spirig, T., Seitz, P., & Vietze, O. (1995). Smart CCD image sensors for optical metrology and machine vision. *Advanced Technologies, Intelligent Vision, 1995.* 11-14.

SRI International (2006). AIC Timeline. Artificial Intelligence Center – SRI International Web site: http://www.ai.sri.com/timeline/

Verdon, P. (2004, Nov. 13). Collimator. Collimator Web site: http://www.timbercon.com/Collimator.html

Vickers, J. (2009). Illumination: getting the basics right. Technical Tips Web site: ftp://ftp2.imaging.de/websites/documents/education/en_GB_Illumination_Intro.pdf

Wang, G., Wu, Y., & Hu, Z. (2002). A novel approach for single view based plane metrology. *16th International Conference on Pattern Recognition, 2002. 2,* 556-559.

Wang, G., Hu, Z., Wu, F., & Tsui, H. T. (2005). Single view metrology from scene constraints. *Image and Vision Computing. 23,* 831-840.

APPENDICES

APPENDIX A

FEATURES OF KEYENCE COMPONENTS:

CV-3002 Series: Multi-camera Universal Machine Vision System

- Similar to a PLC
- 3 Processors
    - RISC CPU chip (reduced instruction set computer)
    - 2 DSP chips (digital signal processor) for image processing
- Memory
    - 15 MB Internal
    - Compact Flash Memory Card Slot
- VGA Output
- 2 Camera Ports
- Terminal Block I/O
    - 9 Output
    - 8 Input Terminals
    - External Triggering Capabilities
- Parallel I/O Connector
- USB Port
- RS-232 Port
- Ethernet Port

CV-035M Series: Double Speed Digital Camera (Monochrome)

- 240000 pixels
- CCD with a double-speed progressive drive method
- 20000 parts per minute
- image transfer time of 16 ms
- “partial image read” allows transfer time of 3 ms

APPENDIX B

DETAILS OF CMM PROGRAM

The test part was located on the platform as follows:

Guide Location and Type: (x,y)

Red Clip: (6,6), (32,17)

Black Cylinder: (15,16), (25,16), (29,10)

An ‘F’ was painted on the left corner of what is considered the Front plane of the test part. The part is always oriented on the table so that this ‘F’ is upright and facing the user. The planes were defined by selecting points to form imaginary rectangles, having heights of only 2 points. The points were selected (looking straight at the plane) from top left to right, then bottom right to left. The Top plane was defined on the side facing upward using 10 points. The Front plane and Side plane were defined using 8 points each. The planes were then intersecting using the software, defining the edges.

The holes were then mapped out by defining 2 circles for each hole. The circles were comprised of 8 points each. To limit variation, and prevent crashing, the points for the top circle of each hole were selected around -0.08”z and the bottom circle around -0.34”z. The points were selected in the following order: N, S, E, W, NW, SE, SW, NE. The defined cylinders were then extended to intersect with the Top plane. At this intersection, the resulting circle was where the hole was measured.

The software was used to create perpendicular construction lines from the intersection of the Top and Front plane to the center of each hole. The length of this line was the width measured. In Excel, this measured width was corrected by subtracting the radius of the corresponding hole, resulting in an edge to edge measurement.

APPENDIX C

PICTURES OF MVS SETUP

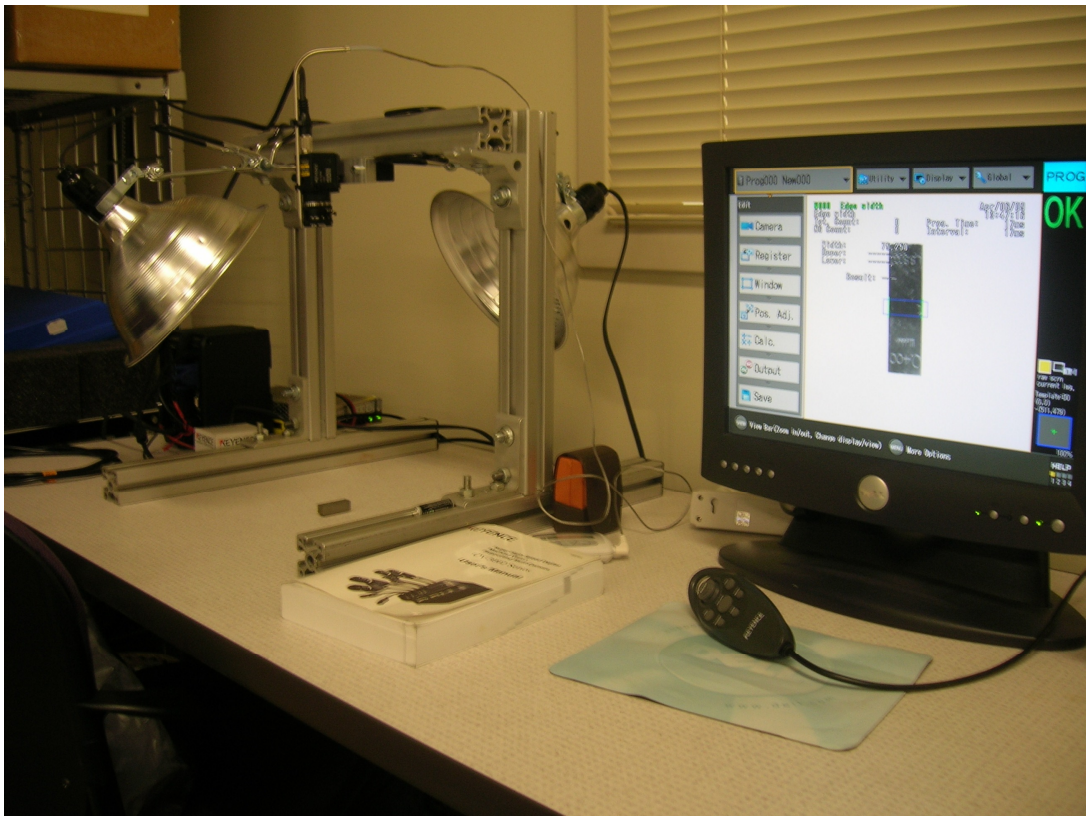

Figure 35 – Complete View

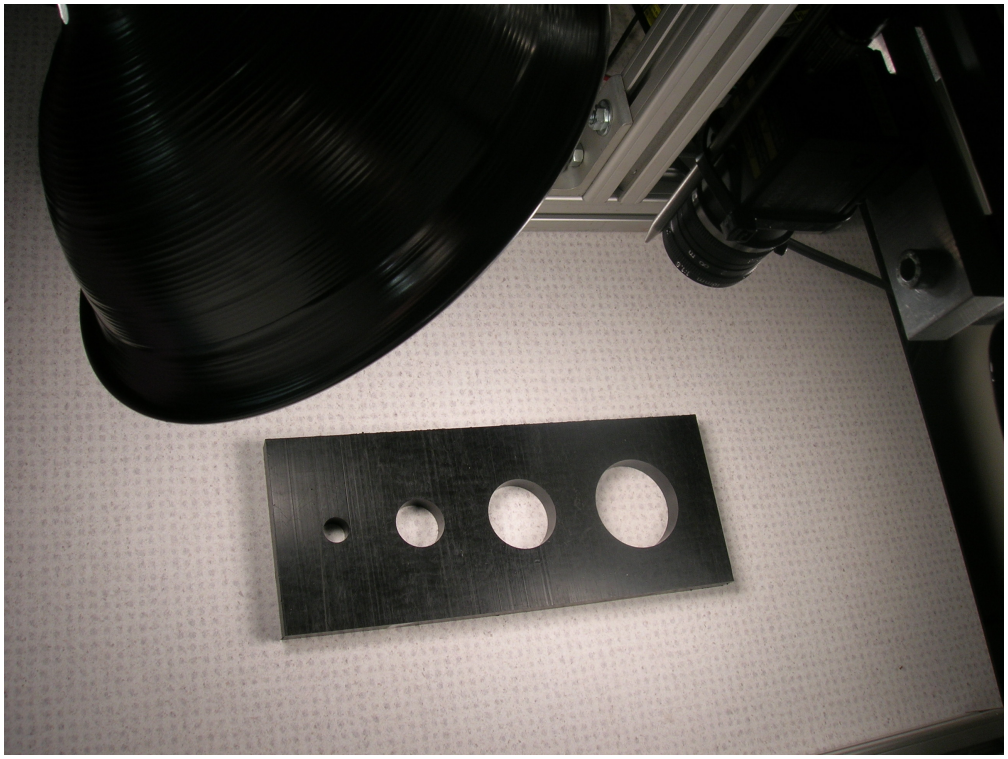

Figure 36 – Overhead with Part

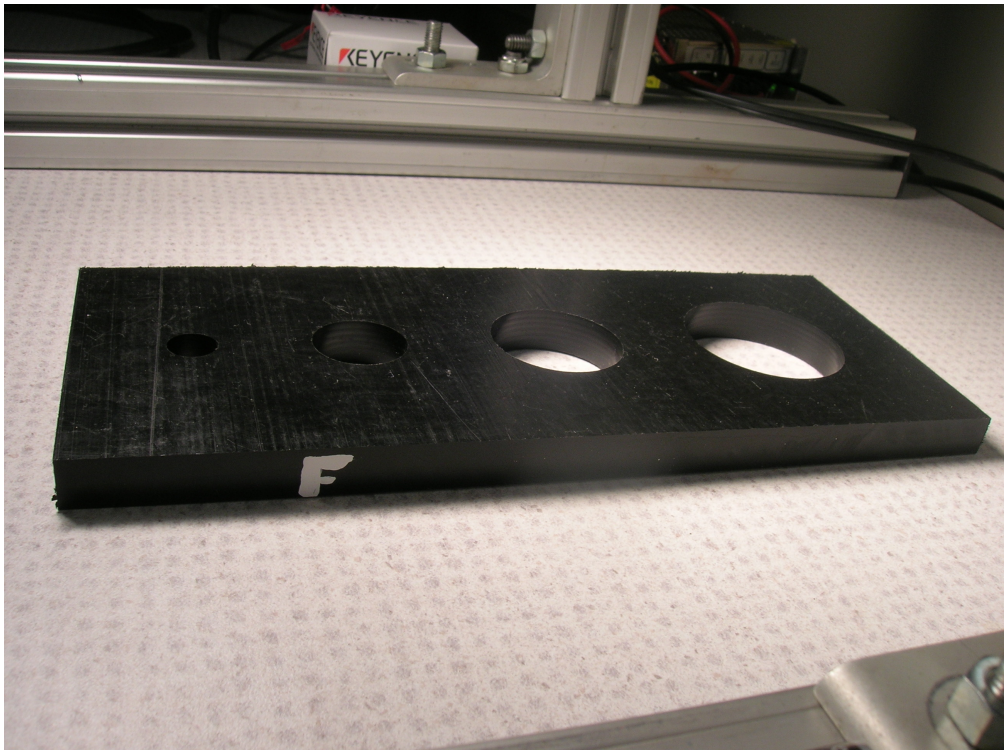

Figure 37 – Close-up of Part

Figure 38 – Camera with Thermometer Probe